Molecular Pharmacology Fast Forward. Published on February 14, 2019 as DOI: 10.1124/mol.118.114710
This article has not been copyedited and formatted. The final version may differ from this version.

Title Page

Statins perturb Gβγ signaling and cell behavior in a Gγ subtype dependent manner

Mithila Tennakoon, Dinesh Kankanamge, Kanishka Senarath, Zehra Fasih and Ajith Karunarathne

From Department of Chemistry and Biochemistry, The University of Toledo, Toledo, OH 43606, USA

Molecular Pharmacology Fast Forward. Published on February 14, 2019 as DOI: 10.1124/mol.118.114710
This article has not been copyedited and formatted. The final version may differ from this version.

Running Title Page

Inhibition of Gβγ signaling by Statins

Corresponding author: Dr. Ajith Karunarathne, Department of Chemistry and Biochemistry, The University of Toledo, 2801 West Bancroft Street, Toledo, OH-43606.

e-mail: Ajith.karunarathne@utoledo.edu

Number of text pages	: 43
Number of tables	: 0
Number of Figures	: 7
Number of References	: 75
Number of words in the Abstract	: 247
Number of words in the Introduction	: 745
Number of words in the Discussion	: 1478

List of nonstandard abbreviations

ARPE-19	- Adult Retinal Pigment Epithelial-19
CHD	- Coronary Heart Disease
CT	- C-terminus
DAG	- Diacylglycerol
DFBS	- Dialyzed fetal bovine serum
DMEM/F-12	- Dulbecco's modified eagle medium/nutrient mixture F-12
FBS	- Fetal bovine serum
FPP	- Farnesyl pyrophosphate
G proteins	- Guanine nucleotide-binding proteins
GGPP	- Geranylgeranyl pyrophosphate

Molecular Pharmacology Fast Forward. Published on February 14, 2019 as DOI: 10.1124/mol.118.114710
This article has not been copyedited and formatted. The final version may differ from this version.

GPCR	- G protein coupled receptor
GRK	- G protein receptor kinases
Gγ	- G protein γ
IM	- Internal membranes
IP3	- Inositol 1, 4, 5-triphosphate
MEM	- Minimum essential medium
Nb80	- Nanobody-80
PI3K	- Phosphatidylinositol-4, 5-bisphosphate 3-kinase
PIP2	- Phosphatidylinositol 4, 5-bisphosphate
PLC β	- Phospholipase C β
PM	- Plasma membrane
RPMI 1640	- Roswell Park Memorial Institute medium
SEM	- Standard error of mean
TIRF	- Total internal reflection
*v*LE	- Leading edge velocity
*v*TE	- Trailing edge velocity
α2-AR	- α2-adrenergic receptor
β1-AR	- β1-adrenergic receptor
mCh	- mCherry

Molecular Pharmacology Fast Forward. Published on February 14, 2019 as DOI: 10.1124/mol.118.114710
This article has not been copyedited and formatted. The final version may differ from this version.

Abstract

Guanine nucleotide-binding proteins (G proteins) facilitate transduction of external signals to the cell interior, regulate a majority of eukaryotic signaling, and thus have become crucial disease drivers. G proteins largely function at the inner leaflet of the plasma membrane (PM) using covalently attached lipid anchors. Both small monomeric and heterotrimeric G proteins are primarily prenylated, either with a 15-carbon farnesyl or a 20-carbon geranylgeranyl polyunsaturated lipid. The mevalonate (HMG-CoA reductase) pathway synthesizes lipids for G protein prenylation. It is also the source of the precursor lipids for many biomolecules including cholesterol. Consequently, the rate-limiting enzymes of the mevalonate pathway are major targets for cholesterol-lowering medications and anti-cancer drug development. Although prenylated G protein γ (Gγ) is essential for G protein coupled receptor (GPCR) mediated signaling, how mevalonate pathway inhibitors, statins, influence subcellular distribution of Gβγ dimer and Gαβγ heterotrimer, as well as their signaling upon GPCR activation, is poorly understood. The present study shows that clinically used statins not only significantly disrupt PM localization of Gβγ, but also perturb GPCR-G protein signaling and associated cell behaviors. The results also demonstrate that the efficiency of prenylation-inhibition by statins is Gγ subtype-dependent and is more effective towards farnesylated Gγ types. Since Gγ is required for Gβγ signaling and it shows a cell and tissue-specific subtype distribution, the present study can help understand the mechanisms underlying clinical outcomes of statins in patients. This work also reveals the potential of statins as clinically usable drugs to control selected GPCR-G protein signaling.

Keywords: Statins, AKT, Alpha-adrenergic receptors, Complement component 5a receptors, Cell migration, Cholesterol, Desensitization, G protein-coupled receptor kinases (GPKs), G protein-coupled receptors (GPCRs), GTP-binding proteins (G proteins), HMG-CoA reductase, Receptor internalization

Molecular Pharmacology Fast Forward. Published on February 14, 2019 as DOI: 10.1124/mol.118.114710
This article has not been copyedited and formatted. The final version may differ from this version.

Introduction

As a major source of morbidity and mortality in developed countries, cardiovascular diseases, specifically Coronary Heart Diseases (CHD), have been on the spotlight for years. The majority of the patients with cardiovascular diseases are diagnosed with atherosclerosis, which is associated with elevated serum cholesterol levels (Gordon and Kannel, 1971; Sytkowski et al., 1990). Although, a fraction of serum cholesterol comes from dietary cholesterol, it is primarily regulated through hepatic cholesterol biosynthesis by the mevalonate pathway (Hajar, 2011) (Fig. 1A). The rate-limiting step of cholesterol biosynthesis in the liver is the conversion of 5- hydroxy-3-methylglutaryl-coenzyme A (HMG-CoA) to mevalonic acid (Rodwell et al., 1976).The enzyme HMG-CoA reductase catalyzes this process (Goldstein and Brown, 1990). Inhibitors of HMG-CoA reductase, also called as statins, are heavily prescribed to reduce serum cholesterol. Initially, statins were identified as secondary metabolites in fungi, and mevastatin is the first natural statin identified (Alberts, 1988; Endo et al., 1976). All statins contain a region that resembles the HMG moiety and thus bind to the active site of the HMG-CoA reductase enzyme (Istvan and Deisenhofer, 2001). As a result, statins reversibly inhibit the enzymatic activity of HMG-CoA reductase and reduce mevalonic acid production (Istvan and Deisenhofer, 2001).

A number of side-effects associated with statin-use including myopathic effects, short-term memory loss, abnormal liver function, glucose intolerance, hyperglycemia, and increased risk for diabetes have been reported (Davies et al., 2016; Golomb and Evans, 2008; Ramkumar et al., 2016). Up to 25% of statin users report muscle symptoms, cramping, soreness and fatigue, thereby forcing many patients to either switch to lower doses, lower potency statins, or to withdraw (Carris et al., 2017). Statins are also associated with ocular adverse effects including blurred vision, visual impairment, visual field defect, reduced visual acuity, myopia, hypermetropia, presbyopia, and astigmatism (Machan et al., 2012; Mizranita and Pratisto, 2015). While one retrospective study indicated that all statins are associated with ocular side effects, atorvastatin showed higher incidences of muscle and liver problems (Mizranita and Pratisto, 2015). Higher occurrences of age-related cataracts in patients on statin therapy have been observed (Machan et al.,

Molecular Pharmacology Fast Forward. Published on February 14, 2019 as DOI: 10.1124/mol.118.114710
This article has not been copyedited and formatted. The final version may differ from this version.

2012). Furthermore, chronic cholesterol depletion using statins has impaired human serotonin1A receptor function (Shrivastava et al., 2010).

Besides cholesterol, mevalonate pathway synthesizes several important lipid precursors such as polyisoprenoids and sterols (Miziorko, 2011). Isoprenoid lipids-farnesyl pyrophosphate (FPP) and geranylgeranyl pyrophosphate (GGPP)- provide membrane anchoring abilities to many proteins and thus are required for numerous functions including cytoskeletal reorganization, differentiation and proliferation (Buhaescu and Izzedine, 2007; Casey, 1992; Chan et al., 2003). FPP and GGPP are precursor-lipids for G proteins prenylation. GPCRs and G proteins govern numerous biological processes and have become therapeutic targets in areas including cancer, cardiac dysfunction, diabetes, central nervous system disorders, obesity, inflammation, vision, and pain. G protein mediated signaling process consists of GPCRs, heterotrimeric G proteins; Gα, Gβγ, and their effectors. Gα and Gβγ act as switches that transmit information from cell surface receptors to intracellular effectors. N- and C-termini (NT and CT) of Gα and Gγ respectively are post-translationally modified with lipid anchors, facilitating heterotrimer formation, and their anchoring to the plasma membrane (PM). N-myristoylation and N-palmitoylation mediate Gα-PM interactions (Chen and Manning, 2001). We showed that distinct PM-interacting properties of 12 mammalian Gγ types are controlled by their CT sequences (Senarath et al., 2018). This sequence comprises a polybasic pre-CaaX region and a CaaX motif (Cook et al., 2006; Watson et al., 1994; Wedegaertner et al., 1995). CaaX motif Cys is prenylated either with a 15-Carbon farnesyl or 20-Carbon geranylgeranyl polyunsaturated lipid anchors (Wedegaertner et al., 1995). Type of prenylation is primarily dictated by the CaaX motif sequence of each Gγ subtype (Wedegaertner et al., 1995) and lipid anchors for prenylation are synthesized by the HMG-CoA pathway (Lacher et al., 2017). Not only Gγ, but many other Ras superfamily G proteins also use prenylation for membrane targeting. How statins perturb Ras members has been extensively studied (Cordle et al., 2005; Dai et al., 2007; Morck et al., 2009). Anti-cancer effects of statins are assigned to their ability to down regulate oncogenic Ras (Chan et al., 2003; Greenwood et al., 2006; Wong et al., 2002). Several studies have suggested that statins reduce isoprenylation of Gγ and subsequently attenuate GPCR signaling (Muhlhauser et al., 2006; Schmechel et al., 2009). However, considering the

Molecular Pharmacology Fast Forward. Published on February 14, 2019 as DOI: 10.1124/mol.118.114710
This article has not been copyedited and formatted. The final version may differ from this version.

necessity of Gγ for Gβγ signaling, and their diverse cell and tissue-wide expression, molecular details including whether statins universally and equally inhibit prenylation of Gγ-members and attenuate GPCR-G protein signaling are not sufficiently explored.

Molecular Pharmacology Fast Forward. Published on February 14, 2019 as DOI: 10.1124/mol.118.114710
This article has not been copyedited and formatted. The final version may differ from this version.

Materials and Methods

Materials

HeLa, ARPE-19, and RAW 264.7 mouse macrophage cell lines were purchased from American Type Culture Collection (Rockville, MD, USA). Cell culture media; minimum essential medium (MEM), Dulbecco's modified eagle medium/nutrient mixture F-12 (DMEM/F-12), and Roswell Park Memorial Institute medium (RPMI 1640) were obtained from Gibco-Thermo Fisher Scientific (Waltham, MA, USA). Fetal bovine serum (FBS) and dialyzed fetal bovine serum (DFBS) were purchased from Atlanta biologicals (Hall County, Georgia, USA). The reagents; Lipofectamine 2000 (Thermofisher), Fluvastatin, Atorvastatin, Lovastatin and Gallein (Cayman Chemical, Ann Arbor, MI), Norepinephrine and isoproterenol hydrochloride (Sigma-Aldrich, St. Louis, MO 63178. USA), C5a (ANASPEC, Fremont, CA, USA), Fluo-4 AM (Molecular probes, Eugene, Oregon), 11-*cis*-retinal (National Eye Institute, Bethesda, MD, USA).

DNA constructs

Blue opsin-mTurquoise, α2-AR-CFP, Akt-PH-mCh, GFP-Gγ9, GFP-Gγ3, Gβ1-YFP, YFP-Gγ2, Gγ4, Gγ5, GFP-Rac1, and untagged K-Ras and M-Ras were kindly provided by Professor N. Gautam's lab, Washington University, St. Louis, Missouri. mCh was amplified from Akt-PH-mCh with NheI and HindIII restriction sites and performed the restriction digestion of both Ras isoforms (vector: untagged K-Ras and M-Ras) and amplified mCh (insert). Digested insert and vectors were ligated and chemically transformed to generate N-terminally mCh tagged K-Ras and M-Ras constructs. Nb80 was kindly provided by Dr. Roshanak Irannejad, University of California, San Francisco, California. To generate the Nb80-mCh construct, GRK2-mCh was digested with BamHI and XbaI to remove GRK2. PCR product of Nb80 was then inserted into remaining mCh vector backbone finally producing Nb80-mCh. Venus-GRK3ct was kindly provided by Dr. Nevin Lambert. mCh-Gγ3(C72A) construct was generated by substituting Cys 72 residue in mCh-Gγ3 with an Ala residue employing the overlap PCR method.

Molecular Pharmacology Fast Forward. Published on February 14, 2019 as DOI: 10.1124/mol.118.114710
This article has not been copyedited and formatted. The final version may differ from this version.

Cell culture and Transfections

HeLa cells were cultured in MEM /10% DFBS/ 1% penicillin–streptomycin medium in a humidified 5% CO_2 incubator at 37°C. RAW 264.7 cells were cultured in RPMI 1640 /10% DFBS with 1% penicillin–streptomycin and ARPE-19 cells were cultured in DMEM/F-12/10% FBS/ with 1% penicillin–streptomycin. At 70-80% confluency, the growth medium was aspirated, and cells were incubated with versene-EDTA (CellGro) for 2 min at 37°C. After the incubation, cells were lifted and centrifuged at 1000g for 3 minutes. Versene-EDTA was then aspirated, and the cell pellet was resuspended in the growth medium and seeded on glass-bottomed dishes (In Vitro Scientific) with a 1×10^5/ml cell density. The following day, after seeding, Lipofectamine 2000 mediated transfection was performed according to the manufacturer's instructions. After 3.5 hours of transfection, cells were replenished with the growth medium containing either dimethyl sulfoxide (DMSO) or respective statins. The next day, live cell imaging was performed.

Live cell imaging, confocal microscopy and data analysis

An imaging system composed of a Nikon Ti-R/B inverted TIRF microscope, a Yokogawa CSU-X1 spinning disk unit (5000 rpm), an Andor FRAP-PA (fluorescence recovery after photo-bleaching and photo-activation) module and iXon ULTRA 897BV back illuminated deep-cooled EMCCD camera was used for live cell imaging and well as optogenetics experiments. Grayscale confocal images were captured on to 512 x 512 pixel CCD with 16 X 16 μm2 pixel size. Pixel depths of the active area and gain register were respectively 180,000 e- and 800,000 e-. Images were acquired with 50 ms exposure with 4-frame averaging. The EM gain was set for 300. Four, 40−100 mW 445 nm, 488 nm, 515 nm, and 594 nm solid-state lasers and an acousto-optical tunable filter (AOTF) were used for excitation, optical activation (OA) as well as photobleaching. Live cell imaging was performed using 60X, 1.4 NA (numerical aperture) oil objective. Emission filters; 478 ±20 nm (Cyan Fluorescent Protein-CFP, mTurquoise), 488 ±20 nm (enhanced Green Fluorescence Protein-eGFP), 542 ±30 nm (Yellow Fluorescent Protein-YFP, and Venus) and 630 ±30 nm (mCherry) were used respectively with 445 nm (~40 μW), 488 nm (~30 μW), 515 nm (~20 μW) and 595

Molecular Pharmacology Fast Forward. Published on February 14, 2019 as DOI: 10.1124/mol.118.114710
This article has not been copyedited and formatted. The final version may differ from this version.

nm (~60 μW) excitation lasers. The power listed was measured at the focal plane of the 60X objective using 1 cm^2 sensor (Ophir PD300). For optical activation of blue opsin using the FRAPPA raster scanning, selected regions of cells were exposed to 445 nm (0.2-1.0 μW at the objective) light. Before OA, cells were incubated with 50 μM 11-cis-retinal for 3-5 min in dark. Digital image analysis was performed using Andor iQ 3.1 software and color values were normalized using in-built Look Up Table tools maintaining a approximately constant setting for each fluorescence sensors. Fluorescence intensities obtained from regions of interest (PM, IMs, and cytosol) were baseline normalized using the intensity of the background. Normalized data were then plotted using Origin pro (OriginLab Corporation). Results of all quantitative assays (Gβγ translocation, PIP2 hydrolysis, and calcium responses) in time-curves were expressed with the standard error of the mean (SEM) from n number of cells (indicated in the figure legends).

Intracellular Ca^{2+} measurements

To measure cytosolic Ca^{2+}, RAW 264.7 cells were cultured on glass-bottomed dishes with RPMI 1640/ DFBS at 37 ^{0}C with 5% CO_2 as described in cell culture and transfections. Experiments were performed two days after seeding cells on glass-bottomed dishes. The day after the seeding, cells were treated with 10 μM fluvastatin and incubated overnight in the 37 ^{0}C incubator with 5% CO_2. The following day, cells were washed twice with 1% (V/V) HBSS containing $NaHCO_3$ and Ca^{2+} (pH 7.2) supplemented with 10 μM fluvastatin. Washed cells were then incubated for 30 min at room temperature with a fluorescent calcium indicator, Fluo-4 AM (2.28 μM) and supplemented with 10 μM fluvastatin in dark conditions. Before start imaging, cells were again washed twice with 1% (V/V) HBSS containing $NaHCO_3$, Ca^{2+} and 10 μM fluvastatin to remove excess Fluo-4 AM. Processed cells were imaged to capture fluorescent intensity of Fluo-4 AM (488 nm) at 1 s intervals using 488 nm excitation-515 nm emission after addition of 20 μM c5a to activate endogenous c5a receptors. The control cells were treated with the vehicle solvent; DMSO, and imaged the same way as fluvastatin-treated cells.

Molecular Pharmacology Fast Forward. Published on February 14, 2019 as DOI: 10.1124/mol.118.114710
This article has not been copyedited and formatted. The final version may differ from this version.

Western blot analysis

After 12-hour incubation, either with carrier solvent (DMSO) or fluvastatin (2 μM), RAW 264.7 cells were exposed to 12.5 μM c5a for 30 mins to activate endogenous c5aR. After the incubation, cells were lysed and the whole cell lysate was subjected to SDS polyacrylamide gel electrophoresis to separate proteins. Proteins were transferred to a PVDF membrane. After blocking with 5% non-fat milk, the membrane was incubated with the primary antibodies specific for p-Akt, t-Akt and β-Actin (Cell Signaling: #4060S, Santa Cruz: sc-5298, sc-47778) overnight at 4 ^{0}C. The next day, the membrane was incubated with the appropriate HRP-conjugated secondary antibodies (Bio-Rad: #1705047, #1705046) at room temperature for 2 hours. After incubating with chemiluminescent detection solutions, the membrane was exposed to an X-ray film. The protein band intensities on X-ray films were quantified and normalized to the level of β-Actin. Experiments were performed in triplicates with independent biological replicates, and quantification and statistical analysis were performed.

Transwell invasion assay

Transwell invasion chambers (with 8 μm membrane pores) were coated with 1x Matrigel (100 μl). The next day, RAW 264.7 cells pre-incubated either with DMSO, Fluvastatin (2 μM), Rho-A inhibitors (EHop-016 – 5 μM, EHT1864- 10 μM, GSK269962- 12.5 μM) or Wortmannin (50 nM) for 24 hours were transferred on top of Matrigel-coated invasion chambers in serum free RPMI (5 x 10^4 cells/well). In Transwell chambers also, cells were treated with either DMSO or the above inhibitors. To asymmetrically activate endogenous c5aR, RPMI containing 10% DFBS with 12.5 μM c5a was added to the lower chambers. After incubation for 24 hours at 37 ^{0}C and 5% CO_2, the invaded cells on the lower surface of the insert membrane were fixed and stained using the Fisher HealthCare™ PROTOCOL™ Hema 3™ Fixative and Solutions (FisherScientific) according to the manufacturer's protocol. The number of invaded cells were counted under a light microscope at 200X total magnification. Every experiment was performed in triplicate and all experiments were repeated four times over different days.

Molecular Pharmacology Fast Forward. Published on February 14, 2019 as DOI: 10.1124/mol.118.114710
This article has not been copyedited and formatted. The final version may differ from this version.

Statistics and reproducibility

Results of all quantitative assays (Gβγ translocation, PIP3 generation, cell migration, and Ca^{2+} response) were calculated as the mean ± standard error of the mean (SEM) or standard deviation (SD) with the listed number of cells in the figure legends from multiple independent experiments (>3). $P < 0.05$ was considered as the threshold for the statistical significance. Comparison of distinct cellular conditions such as Gγ9 and Gγ3 cells and (or) exposed to several statins were performed using one or two-way ANOVA to assess statistical significance. Statistical analysis of data including Ca^{2+} and G protein translocation responses for control and statin-treated cells were performed using two-tailed unpaired t-test. $P< 0.05$ was considered significant. Both Ca2+ and Western blot analysis data were presented as mean ± standard deviation (SD).

Molecular Pharmacology Fast Forward. Published on February 14, 2019 as DOI: 10.1124/mol.118.114710
This article has not been copyedited and formatted. The final version may differ from this version.

Results

Statins disrupt PM localization and signaling of endogenous Gβγ in HeLa cells:

The goal was to examine if statins interrupt the PM localization of endogenous Gβγ and their signaling activation by GPCRs in HeLa cells. Cells were transfected with Gβ1-YFP by incubating cells with transfection medium containing lipofectamine 2000 reagent for 3.5 hours, and subsequently cells were transferred to the regular culture medium, additionally containing statins, i.e. fluvastatin (2 μM), lovastatin (2 μM) or atorvastatin (20 μM) for 12 hours. These concentrations were selected considering their IC50 values (Martin-Navarro et al., 2013). In place of statins, control cells were treated with DMSO, the vehicle solvent of statins. Confocal time-lapse images of cells were captured using a 60X objective with a 1.49 NA. Subcellular distribution of GFP-Gβ1 was captured using 488 nm excitation and 515 nm emission. Cells treated with fluvastatin (+Flu) exhibited primarily a cytosolic Gβ1 distribution (Fig.1B, bottom), while control cells showed primarily a PM and a somewhat internal membrane (IM) distribution (Fig. 1B, top). Cytosolic GFP-Gβ1 distribution indicates that the associated Gγ lacks the prenyl modification at the Cys residue of the CaaX motif. Prenylated Gβγ usually resides either on the PM or IMs. To obtain a numerical value to quantify the extent of inhibition of PM localization, the ratio between fluorescence intensities of Gβ1-YFP on the PM and cytosol ($F_{PM/Cytosol}$) was calculated. A line profile of fluorescence intensities across the PM to the cytosol was measured (Fig 1B, cartoon and plot) and average fluorescence intensities on the PM and cytosol were calculated. Calculations showed that $F_{PM/Cytosol} \leq 1$ for cells with completely inhibited PM localization of Gβγ and $F_{PM/Cytosol} > 1$ for cells with a partial to no inhibition. Deviation of $F_{PM/Cytosol}$ of a treated cell from its control represents the extent of the presence of cytosolic Gβγ, indicating the extent of presumptive prenylation inhibition. For Gβ1 distribution, $F_{PM/Cytosol}$ was 1.04±0.09 for +Flu cells (Fig. 1B, bar graph). The images show that in the +Flu cell, a distinguishable PM region is lacking since fluorescence in the cytosol and the PM are nearly similar. The plot shows the steep drop in the intensity (red curve) at the edge of the cell to the level of the extracellular background. Overall, contrary to the

Molecular Pharmacology Fast Forward. Published on February 14, 2019 as DOI: 10.1124/mol.118.114710
This article has not been copyedited and formatted. The final version may differ from this version.

control cell, +Flu data suggest strong prenylation inhibition by fluvastatin. Next, the effect of fluvastatin on availability of G protein heterotrimers to be activated by GPCR was examined using GPCR activation induced Gβ1γ translocation. We have previously shown that, upon GPCR activation Gβγ translocate from the PM to IMs (Ajith Karunarathne et al., 2012) (Fig. 1C, cartoon). Control HeLa cells exhibited a robust translocation of Gβ1-YFP upon activation of endogenous α2-ARs with 100 μM norepinephrine (Fig. 1C, top panel and plot). However, +Flu cells exhibited 42.85 % attenuated translocation (Fig. 1C, bottom panel and plot). This suggests it is likely that fluvastatin disrupts endogenous Gγ prenylation and thereby attenuates heterotrimer formation as well as Gβγ translocation.

Fluvastatin-induced inhibition of Gγ PM localization is Gγ identity dependent:

The goal was to examine whether fluvastatin equally and universally inhibits PM localization of all Gγ types. This is crucial since Gγ shows a cell and tissue type specific distribution (Cali et al., 1992). Compared to the control HeLa cells, which exhibited GFP-Gγ9 distribution on the PM, +Flu cells exhibited a completely cytosolic GFP-Gγ9 distribution (Fig.2A, left images and bar graph). Upon activation of endogenous α2-AR, control cells exhibited a robust translocation of GFP-Gγ9 to IMs indicating G protein activation and heterotrimer dissociation (Fig. 2A, +NE-top images and plot). On the contrary, fluvastatin treated cells exhibited only a minor increase in their already cytosolic GFP-Gγ9 after α2-AR activation (Fig. 2A, +NE, +Flu images and plot). Like Gγ9, control HeLa cells expressing geranylgeranylated GFP-Gγ3 also showed a prominent PM distribution (Fig. 2B, bottom left and bar graph). Even after 12-hour exposure to fluvastatin, Gγ3 was primarily seen on the PM and only a minor cytosolic distribution was observed (Fig. 2B, middle left and bar graph). This nearly unperturbed PM-bound GFP-Gγ3 fluorescence in fluvastatin treated cells indicated that perhaps a considerable population of Gγ3 is still prenylated. Activation of endogenous α2-AR receptors in both +Flu and control cells exhibited GFP-Gγ3 translocation from the PM to IMs, however exhibited a 1/3 lower magnitude in +Flu cells (Fig. 2B, plot). These data suggest that fluvastatin is likely to attenuate prenylations of Gγ3 to a level that induces a detectable

Molecular Pharmacology Fast Forward. Published on February 14, 2019 as DOI: 10.1124/mol.118.114710
This article has not been copyedited and formatted. The final version may differ from this version.

reduction of heterotrimer activation and free Gβγ translocation. To validate that the remaining PM-bound fraction of Gγ observed after fluvastatin treatment is still prenylated, subcellular distribution of a prenylation deficient Gγ3 mutant was examined. We generated Gγ3(C72A) mutant to eliminate its prenylation, and in HeLa cells, this mutant exhibited completely a cytosolic distribution (Supplemental Figure 1A). This Gγ distribution was similar to the Gγ9 distribution observed in +Flu cells. Therefore, we anticipated that membrane bound Gγ are prenylated and cytosolic Gγ lacks prenylation.

To confirm that statins inhibit membrane attachment of Gγ by inhibiting mevalonate synthesis, HeLa cells expressing either GFP-Gγ3 or GFP-Gγ9 were exposed to fluvastatin (2 μM) for 12 hours, in the presence and absence of mevalonate (0.5 mM). Contrary to control cells exposed to fluvastatin alone, Gγ9 and Gγ3 in +Flu and mevalonate treated cells showed completely a PM distribution (Fig. 2A and 2B, middle and bottom). These cells also exhibited translocation like untreated cells upon endogenous α2-AR activation (Fig. 2A and 2B, plots). However, +Flu cells exhibited a 10 folds lower extent of translocation for Gγ9 and ~2 fold lower for Gγ3 than the respective control cells. Additionally, Gγ9 distribution in cells exposed to farnesyl transferase inhibitor, lonafarnib, is similar to that of fluvastatin treated cells (Supplemental Figure 1E). These data collectively show that fluvastatin induced inhibition of Gγ membrane-anchoring is due to inhibition of mevalonate and subsequent reduction of isoprenyl pyrophosphate synthesis. This data also clearly shows that the observed lack of Gγ PM attachment is not due to a non-specific effect of statins on the cell cycle.

Since Gγ9 and Gγ3 are respectively considered farnesylated and geranylgeranylated based on their CaaX motif sequences, we examined whether the PM interaction of other farnesylated as well as geranylgeranylated Gγ types are similarly disrupted by fluvastatin. Like Gγ9, Gγ1 is also identified as a farnesylated protein and +Flu cells exhibited a completely cytosolic distribution of YFP-Gγ1, while control cells showed a prominent PM distribution (Fig. 3A). Except Gγ1, 9 and 11, other Gγ types are considered primarily geranylgeranylated. Fluvastatin treated Gγ2 expressing cells exhibited a partial inhibition of YFP-Gγ2 membrane attachment (Fig 3B), which is similar to that of Gγ3. Interestingly, compared to Gγ1,

Molecular Pharmacology Fast Forward. Published on February 14, 2019 as DOI: 10.1124/mol.118.114710
This article has not been copyedited and formatted. The final version may differ from this version.

fluvastatin also induced a more pronounced cytosolic distribution of Gγ4 and Gγ5 (Fig. 3C and D). Nevertheless, control cells expressing these Gγ sub-types always exhibited primarily PM distributions (Fig 3A-D). To further support our observation that the PM-localization of farnesylated Gγ types are more effectively inhibited by fluvastatin than geranylgeranylated Gγs, the extent of observed inhibitions in +Flu cells across Gγ types were normalized to their untreated controls (Supplemental Figure 1B). Out of the four Gγ types compared, the highest inhibition of membrane anchorage is observed in Gγ1, while Gγ2, 4 and 5 are less affected by fluvastatin. Overall, the data suggest that presumptively fluvastatin inhibits farnesylation more effectively than geranylgeranylation.

Heterotrimeric G proteins shuttle between the PM and IMs, as heterotrimers at the GPCR-inactive state and as free Gβγ (Ajith Karunarathne et al., 2012). Regardless of the type of Gγ in the heterotrimer, inactive-state shuttling allows heterotrimers to maintain a pool at IMs, while the majority of heterotrimers reside at the PM. To examine whether fluvastatin treatment alters relative PM-IM distribution of heterotrimers, HeLa cells co-transfected with the endoplasmic reticulum (ER) marker, CFP-KDEL and either GFP- Gγ9 or GFP- Gγ3 were exposed to fluvastatin. Unlike control cells which show heterotrimers on the PM and in IMs, both Gγ types were not observed in IMs in +Flu cells. However, CFP-KDEL expression remained unchanged, indicating an intact ER (Supplemental Figure 1C). This indicates that PM is the primary location for heterotrimers and we anticipate that when cells have a surplus heterotrimers, they are docked in IMs. Since fluvastatin treatment is likely to reduce heterotrimer availability, as indicated by universal reduction of Gβγ translocation (Fig. 2), we hypothesize that +Flu cells can accommodate the available heterotrimers at the PM. Additionally the effect of statins on Gα distribution was examined by expressing Gαo-CFP, Gβ1-mCh and Gγ9-YFP in the same cell. Although Gβ1 and Gγ9 showed primarily a cytosolic distribution, Gα stayed PM-bound in most cells. (Supplemental Figure 1D).

Molecular Pharmacology Fast Forward. Published on February 14, 2019 as DOI: 10.1124/mol.118.114710
This article has not been copyedited and formatted. The final version may differ from this version.

The mitigation-potentials of G protein-membrane interactions of different statins are diverse:

How different statins perturb G protein-membrane interactions presumptively by reducing G protein prenylation was comparatively examined. In place of 2 μM fluvastatin, HeLa cells were exposed to either 2 μM lovastatin or 20 μM atorvastatin and their effect on GFP-Gγ9 or GFP-Gγ3 distribution in HeLa cells were examined(Martin-Navarro et al., 2013) (Fig. 4A, top panel and plot). A two-way ANOVA shows that Gγ3 and Gγ9 responses to statins significantly differ, $F(1,12) = 41.2$, $p < 0.05$, such that the average inhibition was significantly higher for Gγ9 (M(mean) = 51.2%, SEM = 10.8) than for Gγ3 (M = 22.8%, SEM = 5.4). The inhibitory effect on Gγ membrane interactions of drugs were also significant, $F(2, 12) = 63.2$, $p > 0.05$ such that +Flu effect was significantly higher (M = 74.6%, SEM = 10.5), compared to Lov (M = 28.1%, SEM = 7.5) and Ator (M = 19.0%, SEM = 3.4). The interaction effect was significant too, $F(2, 12) = 8.5$, $p < 0.05$, where Flu on Gγ9 (M = 92.0%, SEM = 1.0) and Flu on Gγ3 (M = 49.0%, SEM = 1.0) show the highest effect while Ator on Gγ3 (M = 17.0%, SEM = 3.7) and Lov on Gγ3 (M = 11.0%, SEM = 1.0) exhibit the lowest effect. Collectively, this analysis shows that Gγ9 and Gγ3 responded to drug treatments differently. Also, at the same confidence level, three drugs influenced each Gγ types differentially. Although, the difference between influences of lovastatin and atorvastatin on each Gγ types are not significant, they both differ from fluvastatin, i.e. the presumed Gγ prenylation inhibition potential of both atorvastatin and lovastatin is significantly lower than fluvastatin.

Whether these statins also attenuate α2-AR activation induced GFP-Gγ3 or Gγ9 translocation from the PM to IMs was examined (Supplemental Figure 1E). A one-way ANOVA shows that the inhibitory effects of statins on Gγ9 translocations were significant, $F(3, 65) = 30.53$, $p < 0.05$. The inhibitory effects of +Flu and +Lov were significant, where (M = 1.01, SEM = 0.06) and (M = 1.04, SEM = 0.21) respectively, while the effect of +Ator was not significant (M=1.40, SEM = 0.21). A one-way ANOVA with $F(3, 86) = 9.74$, $p < 0.05$ for the inhibitory effects of statins on Gγ3 translocation was significant. +Flu on Gγ3 translocation (M = 1.16, SEM = 0.11) and +Ator (M = 1.22, SEM = 0.12) were significant while the effect

Molecular Pharmacology Fast Forward. Published on February 14, 2019 as DOI: 10.1124/mol.118.114710
This article has not been copyedited and formatted. The final version may differ from this version.

of +Lov (M = 1.36, SEM = 0.24) was not significant. These data collectively suggest that different statins possess distinct abilities to attenuate prenylation of Gγ and thereby the extents of Gβγ translocation.

Next, the ability of fluvastatin, lovastatin and atorvastatin to attenuate prenylation of Ras superfamily members was examined. The majority of the Ras superfamily proteins are prenylated and interact with lipid membranes where they regulate designated biological functions such as cell proliferation and differentiation (Wang and Casey, 2016). The action of the Ras superfamily proteins are tightly regulated and their aberrant behaviors are found in many cancers (Fernandez-Medarde and Santos, 2011). Together with chemotherapeutic agents, statins are prescribed to accelerate tumor cell apoptosis, since they diminish HMG-CoA pathway metabolites, FPP and GGPP, which are required for Ras protein prenylation (Hindler et al., 2006; Yu et al., 2018). HeLa cells incubated with fluvastatin exhibited a near-complete cytosolic distribution of mCh-KRas as well as mCh-MRas respectively indicating their lack of prenyl anchors (Fig. 4B). This inhibition was quantified using the method in Fig. 1B. Control cells incubated with vehicle solvent exhibited primarily PM bound KRas and MRas. At p=0.05, mean $F_{PM/Cytosol}$ ratios of control and +Flu are different where $F_{PM/Cytosol}$ (control)>>1≥ $F_{PM/Cytosol}$ (+Flu). These results were not surprising since both KRas and MRas are considered as farnesylated (Berndt et al., 2011). Interestingly, HeLa cells exposed to lovastatin and atorvastatin exhibited primarily a PM distribution of KRas and MRas (Fig. 4B, bar graph right). Compared to the near-complete inhibition of PM interaction exhibited by fluvastatin, atorvastatin showed ~40% inhibition of MRas and near zero inhibition of KRas while lovastatin exhibited minor inhibition of both Ras members. Collectively these data suggest that, fluvastatin, lovastatin and atorvastatin exhibit distinct prenylation inhibitions of the same Ras protein.

Additionally, prenylation inhibition of small G-protein Rac1 by fluvastatin, lovastatin and atorvastatin was examined in HeLa cells expressing GFP-Rac1. Rac1 being a member of Rho-GTPases, plays a major role in cell migration by contributing to lamellipodia formation (Cotton and Claing, 2009). While the control cells treated with DMSO showed a clear Rac1 distribution on the PM (Fig. 4C, top right image and pie-chart) fluvastatin treated cells exhibited a nuclear localization (Fig. 4C, bottom left image and pie-chart). The extent of inhibition of PM localization of Rac1 by lovastatin and atorvastatin was

Molecular Pharmacology Fast Forward. Published on February 14, 2019 as DOI: 10.1124/mol.118.114710
This article has not been copyedited and formatted. The final version may differ from this version.

significantly lower than fluvastatin. A one-way ANOVA shows that three statins inhibit Rac1 localization at the PM to significantly different extents, $F(2, 6) = 117.5$, $p < 0.01$. Fluvastatin treated cells showed the highest mean inhibition of 99.2 % (SD = 0.5); while lower inhibitions were exhibited by lovastatin (77.0 % ± 7.7), and atorvastatin (25.0% ± 7.2). Additionally, confirming that nuclear-localized Rac1 is unprenylated, cells incubated with lonafarnib (10 μM), a farnesyl transferase inhibitor, also exhibited nuclear localized Rac1-GFP (Supplemental Figure 2A). Moreover, Gγ9 in lonafarnib treated cells were cytosolic as well.

Ramifications of Gβγ signaling in statin-treated cells:

The majority of Gβγ effectors are PM bound or interact with the PM during activation. The goal was to examine whether fluvastatin disrupts Gβγ effector-signaling significantly. Whether the signaling of Gβγ composed of specific Gγ types is more susceptible to be perturbed by fluvastatin was also examined.

(a) Gβγ induced phospholipase C β (PLCβ) activation and subsequent calcium mobilization: Compared to GαqGTP, Gβγ activates PLCβ to a lesser extent, however induces phosphatidylinositol 4, 5-bisphosphate (PIP2) hydrolysis, generating diacylglycerol (DAG) and inositol 1, 4, 5-triphosphate (IP3) (Park et al., 1993). We previously demonstrated that upon activation Gi-coupled α2-AR using norepinephrine, activates PLCβ and induces calcium mobilization (Gupta et al., 2017). Since our data show that statins reduce concentration of PM-interacting Gβγ at near-complete to partial levels, we examined the effect of statins on Gβγ-governed calcium mobilization response. RAW 264.7 cells incubated with either 10 μM fluvastatin, 20 μM atorvastatin or 10 μM lovastatin for 12 hours were pre-treated with the small molecule calcium indicator fluo-4 AM (2.28 μM). Calcium imaging was performed as described before (Siripurapu et al., 2017). After baseline fluo-4 fluorescence was captured, endogenous c5a receptors were activated with 20 μM c5a and fluo4 imaging was continued. A one-way ANOVA that yielded $F(3, 36) = 157.3$, $p < 0.05$ shows that compared to the control cells in which 55.3 % (SD = 5.7) cells showed c5A receptor activation induced calcium responses, fluvastatin treated cells showed a significant inhibition of

Molecular Pharmacology Fast Forward. Published on February 14, 2019 as DOI: 10.1124/mol.118.114710
This article has not been copyedited and formatted. The final version may differ from this version.

the response with a mean difference of 40.2 % (SEM = 2.0) cells (Fig.5A, images and bar graph). Not only the % number of cells with calcium increase (15.1% ±5.3) was reduced in fluvastatin treated cells, the relative response magnitude was also reduced (Fig. 5A, plot). Lovastatin was able to show a minor inhibition of calcium response while inhibition by atorvastatin was insignificant.

(b) Gβγ mediated activation of PI3K, subsequent PIP3 generation and cell migration: Subsequently examined was whether presumptive partial prenylation inhibition of geranylgeranylated Gγ types in RAW 264.7 cells by statins is translated into a reduction in signaling. We have demonstrated that farnesylated Gγ types, including Gγ9, attenuate Gβγ-effectors PLCβ and phosphatidylinositol-4, 5-bisphosphate 3-kinase (PI3K) activations, while geranylgeranylated Gγ types enhance their signaling (Senarath et al., 2018). We also showed that endogenously expressed Gγ3 in RAW cells are required for Gi pathway activation mediated PIP3 production and PLCβ activation during cell migration (Senarath et al., 2018; Siripurapu et al., 2017). In migratory cells, lamellipodia formation at the leading edge is driven by PIP3 produced as a result of Gβγ mediated PI3K activation (Kolsch et al., 2008). In order to interact with Gβγ, p110 subunit of PI3K translocates from the cytosol to the PM and subsequently catalyzes PIP3 production (Braselmann et al., 1997; Brock et al., 2003). We employed the translocation of fluorescently tagged PIP3 sensor (Akt-PH-mCh) from cytosol to the PM to measure PIP3 production. RAW 264.7 cells were transfected with blue opsin- mTurquoise (a Gi-coupled GPCR), Akt-PH-mCh and either GFP-GPI (WT) or GFP-Gγ3. Cells were exposed to either fluvastatin (2 μM), lovastatin (2 μM) or atorvastatin (20 μM) for 12 hours after transfection. Both WT-control and Gγ3-control RAW264.7 cells were treated with DMSO. Cells were supplemented with 11-*cis*-retinal (50 μM) to generate light sensing blue opsin and imaging of GFP using the 488 nm light activated opsin. Plots (Fig. 5B) and two-way ANOVA show that PIP3 responses observed in WT or Gγ3 cells upon blue opsin activation were not significantly different ($F(1, 57) = -0.026$, $p = 1$). Also, selected drugs to inhibit PIP3 production in WT or Gγ3 cells were not significantly different ($F(4, 57) = 0.754$, $p = 0.56$). However, all three drugs exhibited significant differences in their PIP3 response

Molecular Pharmacology Fast Forward. Published on February 14, 2019 as DOI: 10.1124/mol.118.114710
This article has not been copyedited and formatted. The final version may differ from this version.

both in WT and Gγ3 cells ($F(4, 57) = 5.40$ $p < 0.01$) such that compared to WT-control and Gγ3-control cells, fluvastatin treated cells showed respectively a ~73% and a ~82% reductions in PIP3 production. Similarly, lovastatin showed a 38% and 58%, and atorvastatin exhibited 13% and 79% reductions in WT and Gγ3-control cells respectively.

We next examined if the observed reduction of PIP3 generation in fluvastatin treated RAW 264.7 cells also impairs optically-directed migration through localized activation of blue opsin to activate Gi-pathway. Blue opsin in localized regions of RAW 264.7 cells (Fig. 6A-blue box) pre-reconstituted with 11-*cis*-retinal was activated using blue light, and cells exhibited directional migration towards the optical stimuli. Compared to the migration of the leading edge of control cells (6.8 μM ± 0.8), which also exhibited a robust lamellipodia formation and PIP3 production (Fig. 6A-yellow arrow), cells exposed to 10 μM fluvastatin exhibited significantly reduced ($p<0.05$) migration (2.2 μM ± 0.2, (Fig. 6A, bar graph). Fluvastatin treated cells showed a significantly attenuated PIP3 generation, ascertaining the data obtained for PIP3 generation after global activation of opsins (Fig. 5B- yellow arrow). Trailing edge migration of fluvastatin treated cells also exhibited a significantly reduced ($p<0.05$) migration compared to the control cells.

Cell migration and invasion plays a critical role in cancer cell progression and subsequent cancer metastasis (Kirui et al., 2010). The role of Gβγ signaling in cell migration and invasion is thoroughly investigated and well documented (Kim et al., 2012; Kirui et al., 2010; Tang et al., 2011; Vazquez-Prado et al., 2016). In addition to PI3K, Gβγ signaling also contributes to full activation of PIP3-dependent Rac exchanger 1 (P-Rex1) and thus to Rac1 mediated cell mobility (Dbouk et al., 2012; Kim et al., 2012). Blockade of Gβγ is found to diminish cancer metastasis (Tang et al., 2011). Therefore, the ability of fluvastatin to perturb cell invasion was tested by employing Transwell invasion assay for control, as well as fluvastatin (2 μM), Rho-A inhibitors (EHop-016 – 5 μM, EHT1864- 10 μM, GSK269962- 12.5 μM) or wortmannin (50 nM) treated cells for 24 hours. Compared to the number of cells invaded in control, a one-way ANOVA with F (3, 9)=24, $p<0.01$ shows that all three treatments significantly inhibited number of

Molecular Pharmacology Fast Forward. Published on February 14, 2019 as DOI: 10.1124/mol.118.114710
This article has not been copyedited and formatted. The final version may differ from this version.

cells invaded (Fig. 6B). Fluvastatin, RhoA inhibitors and wortmannin exhibited, respectively ~11-fold, 75-fold and 6-fold reductions in their invasion. The higher reduction in cell invasion by fluvastatin compared to wortmannin can be attributed to the ability of fluvastatin to attenuate PM localization of both Gβγ as well as Rho GTPases such as Rac1, which facilitate cell migration.

(c) Fluvastatin exposure attenuates downstream signaling of Gβγ: Akt/PKB pathway is one of the major signaling networks activated by Gβγ. Gβγ induced phosphorylation of the PI3K and subsequent PIP3 generation recruits Akt to the PM. Activated Akt triggers numerous downstream responses including cell survival, proliferation, growth and cell migration (Hemmings and Restuccia, 2015). Since our data shows that fluvastatin treatment diminishes Gβγ-mediated PI3K/PIP3 signaling and Akt links Gβγ with cell migration and invasion, Western blot analysis was employed to examine the effect of fluvastatin on Akt phosphorylation. Raw264.7 cells were incubated either with 2 μM fluvatatin or DMSO, for 24 hours. Cells were lysed and extracted proteins were separated using SDS-PAGE. Western blot analysis was performed using standard protocols and total Akt, phospho-Akt and actin was detected using specific primary and secondary antibodies. The phospho-Akt level was normalized to expression levels of both total-Akt and β-actin. Interestingly the data revealed a two-fold reduction in Akt phosphorylation compared to the DMSO-treated control cells (Fig. 6C, Supplemental Figure 2B). This data further confirms the ability of fluvastatin to inhibit Gβγ signaling and Gβγ-mediated downstream cellular events.

Fluvastatin suppresses internalization of activated β1 adrenergic receptors:

Desensitization of activated GPCRs protects cells from excessive signaling and is achieved by the receptor internalization (van Koppen and Jakobs, 2004). G protein receptor kinases (GRKs) help physical removal of activated GPCR from the PM by phosphorylating the serine and tyrosine residues in the third cytosolic loop and the CT of the receptor (Evron et al., 2012; van Koppen and Jakobs, 2004). Especially, GRK2 (β-adrenergic receptor kinase 2) phosphorylates agonist-activated β-adrenergic receptors (β1-AR), promoting

Molecular Pharmacology Fast Forward. Published on February 14, 2019 as DOI: 10.1124/mol.118.114710
This article has not been copyedited and formatted. The final version may differ from this version.

GPCR-β-arrestin interactions and subsequent desensitization (Lefkowitz, 1998). GRK2 activity requires binding of Gβγ (Haga and Haga, 1990; Pitcher et al., 1992). Disruption of Gβγ binding domain of GRK2 eliminates this activation-dependent receptor phosphorylation (Carman et al., 2000). Recently, nanobody-80 (Nb80), a conformation-specific single domain antibody for activated β1-AR was employed to monitor active-state β1-AR. Upon activation of β1-AR with its agonist, it has been shown that cytosolic Nb80-GFP translocates to the PM and binds to the agonist bound activated β1-AR. When GRK2 induces internalization of activated β1-AR, bound Nb80 also internalizes and this is indicated by the accumulation of Nb80-GFP fluorescence in IMs (Irannejad et al., 2017) (Fig. 7A, cartoon). Since Gβγ plays a key role in GRK2 mediated receptor internalization, we examined the internalization of activated β1-AR by monitoring subcellular location of Nb80-GFP in the presence and absence (control) of fluvastatin. To confirm Gβγ involvement, additional experiments were performed in the presence of gallein (Gβγ inhibitor) (Casey et al., 2010), and in cells expressing venus-GRK3ct (to sequester Gβγ) (Hollins et al., 2009). HeLa cells expressing β1-AR-CFP and Nb80-GFP were pre-incubated with 5 μM fluvastatin or DMSO for 12 hours. Using 20 μM isoproterenol, β1-AR was activated and the Nb80-GFP recruitment to IMs was monitored (Fig. 7A, images and plot). A one-way ANOVA shows that compared to control cells with the mean normalized IM fluorescence of 2.061± 0.003, fluvastatin show a significantly lower Nb80 recruitment to IMs (1.523± 0.002, ~50%) at $p<0.05$. Even more significant reductions (~80%) were observed in gallein treated cells (1.159 ±0.06) and in GRK3ct expressing cells (1.216 ± 0.002) compared to control cells. Since, the extent of Nb80-recruitment inhibition by fluvastatin is between that of the control and gallein treated as well as GRK3ct cells, fluvastatin mediated Gβγ inhibition in Raw 264.7 cells appears to be partial.

Fluvastatin significantly impairs heterotrimer activation and Gβγ translocation from the PM to IMs in retinal pigment epithelial cells:

Use of statins is associated with ocular diseases including vision impairment, blurred vision and cataract development (Machan et al., 2012; Mizranita and Pratisto, 2015). Visual transduction requires the

Molecular Pharmacology Fast Forward. Published on February 14, 2019 as DOI: 10.1124/mol.118.114710
This article has not been copyedited and formatted. The final version may differ from this version.

activation of G protein heterotrimers by light-activated opsins and cells in the retina primarily employ farnesylated Gγ types (Gγ1 and Gγ9) in heterotrimers. Since statins greatly perturb the PM localization of the farnesylated Gγ types, we examined whether statins reduce Gβγ translocation (which is considered as a measure of heterotrimer activation (Senarath et al., 2016)) in Adult Retinal Pigment Epithelial-19 (ARPE-19) cells. Gγ subtype expression profile of ARPE-19 cells was determined using quantitative real time PCR (qRT-PCR). Data show that the major Gγ subtypes endogenously expressed in ARPE19 cells are Gγ11 and Gγ5 (Fig. 7B, bar graph). Since Gγ11 is farnesylated and possesses a low PM affinity (Ajith Karunarathne et al., 2012), GPCR activation induced translocation of Gβγ in fluvastatin-exposed ARPE-19 was examined. ARPE19 cells were transfected with Gβ1-mCh and α2AR-CFP, while exposing to 2 μM fluvastatin. Control cells treated with DMSO exhibited a prominent distribution of Gβ1-mCh on the PM and IMs, while Gβ1 distribution was completely cytosolic in cells exposed to 2 μM fluvastatin (Fig. 7B, top panel). Similarly, inhibition of membrane distribution of Gγ9 was also examined by transfecting ARPE19 cells with mCh-Gγ9. Like Gβ1, Gγ9 also exhibited a complete cytosolic distribution in cells exposed to fluvastatin while control cells showed a membrane distribution (Fig. 7B, bottom panel). Next, the effect of fluvastatin on heterotrimer activation in ARPE19 cells was investigated by monitoring mCh-Gγ9 as well as Gβ1-mCh translocation from the PM to IMs after activating the transfected α2AR. Analogous to the observations in HeLa cells, both Gβ1 and Gγ9 exhibited a robust translocation from PM to the IM in control cells while fluvastatin treated ARPE-19 cells failed to exhibit detectable translocations of either Gβ1 or Gγ9 (Figure 7B, plots).

Molecular Pharmacology Fast Forward. Published on February 14, 2019 as DOI: 10.1124/mol.118.114710
This article has not been copyedited and formatted. The final version may differ from this version.

Discussion

Statins are globally used as effective lipid-lowering medications, primarily to reduce the risk of cardiovascular diseases and associated mortality. However, several side effects such as myopathy, ocular adverse effects including blurred vision and visual impairment, cognitive effects such as short term memory loss, abnormal liver function, glucose intolerance and increased risk for diabetes are reported in patients treated with statins (Davies et al., 2016; Golomb and Evans, 2008; Mizranita and Pratisto, 2015). Being a competitive inhibitor of the enzyme, HMG-CoA reductase; a crucial enzyme of the mevalonate (or cholesterol synthesis) pathway, statins effectively reduce not only the production of cholesterol but also other lipids including isoprenoids (Miziorko, 2011). Isoprenoids are precursors for the synthesis of prenyl pyrophosphates, which are required for the prenylation of a large cohort of G-proteins. The present study draws a clear link between the use of statins and the perturbation of GPCR and heterotrimeric G-protein signaling, providing potential explanations for some of the side-effects related to statin usage (Golomb and Evans, 2008).

Membrane anchorage is a crucial factor for the functioning of Ras superfamily and heterotrimeric G-proteins. Being able to modulate and prevent the activity of Ras superfamily G-proteins, statins exert several pleiotropic side effects such as reduction of cell proliferation that consequently has expanded its usage as a chemotherapeutic agent (Liao and Laufs, 2005). The data presented in this study exhibit that statins perturb the PM localization of Gγ and thereby Gβγ in a Gγ subtype dependent manner, as a result of the reduction of prenyl anchors required for Gγ prenylation (Hildebrandt, 2011; Wedegaertner et al., 1995). Interestingly, data show that Gγ types that are being prenylated with geranylgeranyl anchors are only partially susceptible to statin-mediated likely inhibition of prenylation. This differential inhibition is also characterized by near-complete inhibition of PM-localization of farnesylated Gγ, attenuating activation of heterotrimers with farnesylated Gγ. The effectiveness of statins to inhibit farnesylation is also evident from

Molecular Pharmacology Fast Forward. Published on February 14, 2019 as DOI: 10.1124/mol.118.114710
This article has not been copyedited and formatted. The final version may differ from this version.

the near-complete inhibition of primarily farnesylation-sensitive Ras family proteins such as KRas, NRas and HRas.

It has been suggested that the CT sequence that determines the type of prenylation is not just limited to CaaX motif (Senarath et al., 2018). Also suggested was the ability of proteins that usually prefer farnesylation can undergo geranylgeranylation, in the presence of farnesyl transferase inhibitors (Whyte et al., 1997). We hypothesized that, Gγ types are not completely farnesylated of geranylgeranylated. Although nine out of twelve Gγ types are primarily identified as geranylgeranylated proteins, to a certain degree they are also farnesylated as well. It appears that the major anchoring type of a Gγ is recognized as the type of prenylation. Our experimental data show varying degrees of likely inhibition Gγ geranylgeranylation upon exposure to statins supporting this hypothesis. For instance, extents of the presence of cytosolic Gγ indicates a minor Gγ2, Gγ3, Gγ4 and Gγ5 prenylation inhibitions. This also suggests that a considerable fraction in Gγ4 as well as Gγ5 are likely to be farnesylated. A larger reduction of NE-induced Gγ3 translocation compared to that of Gβ1 by fluvastatin was observed, although their subcellular distribution data shows a relatively a lesser inhibition of Gγ3 prenylation by fluvastatin. We believe that this is due to partially cytosolic YFP-Gβ1 interfering with the detection of YFP-Gβ1 translocation. The observed differential effects of statins on farnesylated and geranylgeranylated Gγ, likely indicating distinct prenylation inhibition patterns, can be partly due to the higher incidence of GGPP production. This is in addition to the conversion of FPP to GGPP by GGPP synthase. Examination of cholesterol synthesis pathway indicates that, compared to FPP, a cell can have a relatively higher population of GGPP through the direct conversion of isopentenyl-PP to GGPP. Alternatively, in addition to being utilized to produce farnesylated proteins, FPP is also consumed to produce other lipids in the mevalonate pathway, including GGPP and cholesterol. Collectively, these differences can explain why Gγ types differentially susceptible to prenylation inhibition by statins (Fig. 1A). Interestingly, the near-complete inhibition of both Gγ1 and Gγ9 suggests that, in the absence of farnesylation, these Gγ types cannot effectively undergo geranylgeranylation.

Molecular Pharmacology Fast Forward. Published on February 14, 2019 as DOI: 10.1124/mol.118.114710
This article has not been copyedited and formatted. The final version may differ from this version.

Translocation of Gβγ in cells expressing different Gγ subtypes upon the activation of GPCR indicates activation G proteins (Ajith Karunarathne et al., 2012). Attenuated-translocation observed in statin-exposed cells in a Gγ-dependent manner, thus signifies the reduction of heterotrimer activation. Therefore, it is likely that heterotrimeric G protein signaling is similarly perturbed in patients treated with statins. Gγ types show cell and tissue-specific subtype distributions (Cali et al., 1992). Our data therefore suggest that G protein signaling perturbation by statins can differentially influence GPCR-G protein controlled-processes in a tissue and organ function specific manner. Due to the likely-extensive inhibition of Gγ farnesylation by statins, pronounced after effects in tissues and organs that predominantly employ farnesylated Gγ types can be anticipated. For instance, photoreceptor cells in the retina of the eye express Gγ1 and Gγ9 as the major Gγ (Pearring et al., 2013). This unique Gγ expression can be understood by examining the visual transduction in which GTP bound Gα-transducin is the major signal transducer, generated by the activated opsin to trigger cGMP signaling. Here, cells appear to employ Gβγ with farnesylated Gγ due to their low PM affinity to prevent unnecessary as well as potentially deleterious Gβγ signaling for photoreceptor cells. If statins significantly reduce farnesylation, consequently that can reduce transducin-containing heterotrimer formation as well, hampering cGMP pathway activation. They also reported recovery from the effects upon statin discontinuation (Leuschen et al., 2013). These observations are consistent with the ability of statin to temporarily inhibit HMG-CoA. Data from ARPE19 cells with primarily farnesylated endogenous Gγ showed significant inhibition of PM localization and GPCR activation-induced Gβγ translocation upon exposure to fluvastatin. This also indicates the likely after-effects of statins on the vision system. Based on these facts and data, we propose that the dominant expression of farnesylated Gγ types in photoreceptor cells is linked to the occurrence of ocular disorders in the patients using statins.

Several studies have shown interference of immune responses by statins due to the attenuated production of downstream metabolites in HMG-CoA pathway including FPP and GGPPs. Similar to Gγ, these lipids are required for PM-anchoring of small GTPases such as RhoA, Rac, and Ras. Our data show an impairment of their PM-localization in cells exposed to statins. Our data also show that statins induce

Molecular Pharmacology Fast Forward. Published on February 14, 2019 as DOI: 10.1124/mol.118.114710
This article has not been copyedited and formatted. The final version may differ from this version.

perturbation of Gβγ mediated cell migration and invasion, which are critical steps of immune responses and metastasis. Prolonged exposure to statins including fluvastatin has been shown to negatively impact cognitive function (Golomb and Evans, 2008; Ramkumar et al., 2016). Out of 12 gamma subtypes, Gγ2 and Gγ3 are predominant in the brain (Yim et al., 2017), the partial inhibition of their membrane localization by fluvastatin and the consequent perturbation of associated signaling can partially be responsible for the development of cognitive effects in patients using statins. Our previous findings show that Gi-pathway governed PIP3 production is Gγ subtype dependent and Gγ3 is the foremost Gγ that supports PIP3 production (Senarath et al., 2018). Partially delocalized Gγ3 from the PM to the cytosol upon fluvastatin treatment thus explains the attenuation of downstream signaling of Gβγ including Akt phosphorylation, cell migration and invasion.

Cardiac muscle activities are strongly regulated by GPCRs including β-adrenergic, acetylcholine and angiotensin receptors, thus they have become therapeutic targets for cardiovascular diseases (Bathgate-Siryk et al., 2014). Agonist activated cardiac β-adrenergic receptors undergo desensitization upon phosphorylation. This process is controlled by Gβγ and GRKs, attenuating GPCR signaling (Reiter and Lefkowitz, 2006). Upregulation of GRK isoforms such as GRK2 and GRK5 markedly cause chronic heart failures due to reduction of β-adrenergic receptors in cardiac muscles (Lymperopoulos et al., 2012). Patients treated with statins have exhibited substantially lower cardiac problems, including reduced damages from ischemia-reperfusion injury (IRI). Excessive β-adrenergic receptor internalization is a leading cause of IRI (Tilley and Rockman, 2006). Gβγ triggers GRK2-induced β adrenergic receptor phosphorylation, marking it for internalization (Cahill et al., 2017; Ribas et al., 2007), thus Gβγ signaling is deleterious during a myocardial infarction (Tilley and Rockman, 2006). Our data not only show that statins reduce Gβγ signaling, but also exhibit a significant reduction in β-adrenergic receptor desensitization. Our findings therefore suggest added beneficial effects of statin on cardiac function, in addition to their ability to lower cholesterol bio-synthesis.

Molecular Pharmacology Fast Forward. Published on February 14, 2019 as DOI: 10.1124/mol.118.114710
This article has not been copyedited and formatted. The final version may differ from this version.

In summary, we show for the first time that statins perturb GPCR-G protein signaling in a Gγ type dependent manner. Our data conclusively show that, fluvastatin inhibits prenylation of farnesylation-sensitive Gγ strongly. This also suggests that, functions in cells and tissues predominantly expressing these Gγ types are more susceptible to be interfered by statins. Additionally, we show that several crucial Gβγ-controlled cellular processes including chemokine cell migration and internalization of β-adrenergic receptors are significantly attenuated by statins. Our findings also indicate that numerous GPCR-G protein governed cellular functions, whether beneficial or not, are likely to be differentially perturbed by statins, and thus require further investigations.

Molecular Pharmacology Fast Forward. Published on February 14, 2019 as DOI: 10.1124/mol.118.114710
This article has not been copyedited and formatted. The final version may differ from this version.

Acknowledgements

We acknowledge Dr. Deborah Chadee for providing experimental support for the Western blot analysis. We thank Drs. N. Gautam, Roshanak Irannejad and Nevin Lambert respectively for G protein subunit, Nb80 and GRK3ct constructs. We thank National Eye Institute for providing 11-*cis*-retinal. We also thank Kasun Ratnayake and Diniti Welivita for comments. We also thank the Departments; Chemistry and Biochemistry and Biological Sciences at The University of Toledo for providing access to various instrumentation.

Molecular Pharmacology Fast Forward. Published on February 14, 2019 as DOI: 10.1124/mol.118.114710
This article has not been copyedited and formatted. The final version may differ from this version.

Authorship Contributions

Participated in research design: Karunarathne, Tennakoon and Kankanamge

Conducted experiments: Tennakoon, Kankanamge and Senarath

Performed data analysis: Tennakoon, Kankanamge, Senarath and Fasih

Wrote or contributed to the writing of the manuscript: Tennakoon, Karunarathne, Kankanmge, Senarath and Fasih

Molecular Pharmacology Fast Forward. Published on February 14, 2019 as DOI: 10.1124/mol.118.114710
This article has not been copyedited and formatted. The final version may differ from this version.

References

Ajith Karunarathne WK, O'Neill PR, Martinez-Espinosa PL, Kalyanaraman V and Gautam N (2012) All G protein betagamma complexes are capable of translocation on receptor activation. *Biochem Biophys Res Commun* **421**(3): 605-611.

Alberts AW (1988) Discovery, biochemistry and biology of lovastatin. *The American journal of cardiology* **62**(15): 10j-15j.

Bathgate-Siryk A, Dabul S, Pandya K, Walklett K, Rengo G, Cannavo A, De Lucia C, Liccardo D, Gao E, Leosco D, Koch WJ and Lymperopoulos A (2014) Negative impact of beta-arrestin-1 on post-myocardial infarction heart failure via cardiac and adrenal-dependent neurohormonal mechanisms. *Hypertension (Dallas, Tex : 1979)* **63**(2): 404-412.

Berndt N, Hamilton AD and Sebti SM (2011) Targeting protein prenylation for cancer therapy. *Nat Rev Cancer* **11**(11): 775-791.

Braselmann S, Palmer TM and Cook SJ (1997) Signalling enzymes: bursting with potential. *Current biology : CB* **7**(8): R470-473.

Brock C, Schaefer M, Reusch HP, Czupalla C, Michalke M, Spicher K, Schultz G and Nurnberg B (2003) Roles of G beta gamma in membrane recruitment and activation of p110 gamma/p101 phosphoinositide 3-kinase gamma. *J Cell Biol* **160**(1): 89-99.

Buhaescu I and Izzedine H (2007) Mevalonate pathway: a review of clinical and therapeutical implications. *Clin Biochem* **40**(9-10): 575-584.

Cahill TJ, 3rd, Thomsen AR, Tarrasch JT, Plouffe B, Nguyen AH, Yang F, Huang LY, Kahsai AW, Bassoni DL, Gavino BJ, Lamerdin JE, Triest S, Shukla AK, Berger B, Little Jt, Antar A, Blanc A, Qu CX, Chen X, Kawakami K, Inoue A, Aoki J, Steyaert J, Sun JP, Bouvier M, Skiniotis G and Lefkowitz RJ (2017) Distinct conformations of GPCR-beta-arrestin complexes mediate desensitization, signaling, and endocytosis. *Proc Natl Acad Sci U S A* **114**(10): 2562-2567.

Cali JJ, Balcueva EA, Rybalkin I and Robishaw JD (1992) Selective tissue distribution of G protein gamma subunits, including a new form of the gamma subunits identified by cDNA cloning. *The Journal of biological chemistry* **267**(33): 24023-24027.

Carman CV, Barak LS, Chen C, Liu-Chen LY, Onorato JJ, Kennedy SP, Caron MG and Benovic JL (2000) Mutational analysis of Gbetagamma and phospholipid interaction with G protein-coupled receptor kinase 2. *The Journal of biological chemistry* **275**(14): 10443-10452.

Carris NW, Tipparaju SM, Magness DJ, Chapalamadugu KC and Magness RR (2017) Pleiotropic effects of metformin to rescue statin-induced muscle injury and insulin resistance: A proposed mechanism and potential clinical implications. *Medical hypotheses* **107**: 39-44.

Casey LM, Pistner AR, Belmonte SL, Migdalovich D, Stolpnik O, Nwakanma FE, Vorobiof G, Dunaevsky O, Matavel A, Lopes CM, Smrcka AV and Blaxall BC (2010) Small molecule disruption of G beta gamma signaling inhibits the progression of heart failure. *Circulation research* **107**(4): 532-539.

Casey PJ (1992) Biochemistry of protein prenylation. *Journal of lipid research* **33**(12): 1731-1740.

Chan KK, Oza AM and Siu LL (2003) The statins as anticancer agents. *Clinical cancer research : an official journal of the American Association for Cancer Research* **9**(1): 10-19.

Chen CA and Manning DR (2001) Regulation of G proteins by covalent modification. *Oncogene* **20**(13): 1643-1652.

Cook LA, Schey KL, Wilcox MD, Dingus J, Ettling R, Nelson T, Knapp DR and Hildebrandt JD (2006) Proteomic analysis of bovine brain G protein gamma subunit processing heterogeneity. *Molecular & cellular proteomics : MCP* **5**(4): 671-685.

Cordle A, Koenigsknecht-Talboo J, Wilkinson B, Limpert A and Landreth G (2005) Mechanisms of statin-mediated inhibition of small G-protein function. *The Journal of biological chemistry* **280**(40): 34202-34209.

Cotton M and Claing A (2009) G protein-coupled receptors stimulation and the control of cell migration. *Cellular signalling* **21**(7): 1045-1053.

Dai Y, Khanna P, Chen S, Pei XY, Dent P and Grant S (2007) Statins synergistically potentiate 7-hydroxystaurosporine (UCN-01) lethality in human leukemia and myeloma cells by disrupting Ras farnesylation and activation. *Blood* **109**(10): 4415-4423.

Davies JT, Delfino SF, Feinberg CE, Johnson MF, Nappi VL, Olinger JT, Schwab AP and Swanson HI (2016) Current and Emerging Uses of Statins in Clinical Therapeutics: A Review. *Lipid Insights* **9**: 13-29.

Dbouk HA, Vadas O, Shymanets A, Burke JE, Salamon RS, Khalil BD, Barrett MO, Waldo GL, Surve C, Hsueh C, Perisic O, Harteneck C, Shepherd PR, Harden TK, Smrcka AV, Taussig R, Bresnick AR, Nurnberg B, Williams RL and Backer JM (2012) G protein-coupled receptor-mediated activation of p110beta by Gbetagamma is required for cellular transformation and invasiveness. *Science signaling* **5**(253): ra89.

Endo A, Kuroda M and Tsujita Y (1976) ML-236A, ML-236B, and ML-236C, new inhibitors of cholesterogenesis produced by Penicillium citrinium. *The Journal of antibiotics* **29**(12): 1346-1348.

Evron T, Daigle TL and Caron MG (2012) GRK2: multiple roles beyond G protein-coupled receptor desensitization. *Trends Pharmacol Sci* **33**(3): 154-164.

Fernandez-Medarde A and Santos E (2011) Ras in cancer and developmental diseases. *Genes Cancer* **2**(3): 344-358.

Goldstein JL and Brown MS (1990) Regulation of the mevalonate pathway. *Nature* **343**(6257): 425-430.

Golomb BA and Evans MA (2008) Statin adverse effects : a review of the literature and evidence for a mitochondrial mechanism. *Am J Cardiovasc Drugs* **8**(6): 373-418.

Gordon T and Kannel WB (1971) Premature mortality from coronary heart disease. The Framingham study. *Jama* **215**(10): 1617-1625.

Greenwood J, Steinman L and Zamvil SS (2006) Statin therapy and autoimmune disease: from protein prenylation to immunomodulation. *Nature reviews Immunology* **6**(5): 358-370.

Gupta RK, Swain S, Kankanamge D, Priyanka PD, Singh R, Mitra K, Karunarathne A and Giri L (2017) Comparison of Calcium Dynamics and Specific Features for G Protein-Coupled Receptor-Targeting Drugs Using Live Cell Imaging and Automated Analysis. *SLAS discovery : advancing life sciences R & D* **22**(7): 848-858.

Haga K and Haga T (1990) Dual regulation by G proteins of agonist-dependent phosphorylation of muscarinic acetylcholine receptors. *FEBS Letters* **268**(1): 43-47.

Hajar R (2011) Statins: past and present. *Heart views : the official journal of the Gulf Heart Association* **12**(3): 121-127.

Hemmings BA and Restuccia DF (2015) The PI3K-PKB/Akt pathway. *Cold Spring Harbor perspectives in biology* **7**(4).

Hildebrandt JD (2011) 6 - Heterogeneous Prenyl Processing of the Heterotrimeric G protein Gamma Subunits, in *The Enzymes* (Tamanoi F, Hrycyna CA and Bergo MO eds) pp 97-124, Academic Press.

Hindler K, Cleeland CS, Rivera E and Collard CD (2006) The role of statins in cancer therapy. *The oncologist* **11**(3): 306-315.

Hollins B, Kuravi S, Digby GJ and Lambert NA (2009) The c-terminus of GRK3 indicates rapid dissociation of G protein heterotrimers. *Cell Signal* **21**(6): 1015-1021.

Irannejad R, Pessino V, Mika D, Huang B, Wedegaertner PB, Conti M and von Zastrow M (2017) Functional selectivity of GPCR-directed drug action through location bias. *Nat Chem Biol* **13**(7): 799-806.

Istvan ES and Deisenhofer J (2001) Structural mechanism for statin inhibition of HMG-CoA reductase. *Science (New York, NY)* **292**(5519): 1160-1164.

Kim EK, Yun SJ, Ha JM, Kim YW, Jin IH, Woo DH, Lee HS, Ha HK and Bae SS (2012) Synergistic induction of cancer cell migration regulated by Gbetagamma and phosphatidylinositol 3-kinase. *Experimental & molecular medicine* **44**(8): 483-491.

Kirui JK, Xie Y, Wolff DW, Jiang H, Abel PW and Tu Y (2010) Gbetagamma signaling promotes breast cancer cell migration and invasion. *The Journal of pharmacology and experimental therapeutics* **333**(2): 393-403.

Kolsch V, Charest PG and Firtel RA (2008) The regulation of cell motility and chemotaxis by phospholipid signaling. *J Cell Sci* **121**(Pt 5): 551-559.

Lacher SM, Bruttger J, Kalt B, Berthelet J, Rajalingam K, Wortge S and Waisman A (2017) HMG-CoA reductase promotes protein prenylation and therefore is indispensible for T-cell survival. *Cell death & disease* **8**(5): e2824.

Lefkowitz RJ (1998) G protein-coupled receptors. III. New roles for receptor kinases and beta-arrestins in receptor signaling and desensitization. *The Journal of biological chemistry* **273**(30): 18677-18680.

Leuschen J, Mortensen EM, Frei CR, Mansi EA, Panday V and Mansi I (2013) Association of statin use with cataracts: a propensity score-matched analysis. *JAMA ophthalmology* **131**(11): 1427-1434.

Liao JK and Laufs U (2005) Pleiotropic effects of statins. *Annu Rev Pharmacol Toxicol* **45**: 89-118.

Lymperopoulos A, Rengo G and Koch WJ (2012) GRK2 inhibition in heart failure: something old, something new. *Current pharmaceutical design* **18**(2): 186-191.

Machan CM, Hrynchak PK and Irving EL (2012) Age-related cataract is associated with type 2 diabetes and statin use. *Optometry and vision science : official publication of the American Academy of Optometry* **89**(8): 1165-1171.

Martin-Navarro CM, Lorenzo-Morales J, Machin RP, Lopez-Arencibia A, Garcia-Castellano JM, de Fuentes I, Loftus B, Maciver SK, Valladares B and Pinero JE (2013) Inhibition of 3-hydroxy-3-methylglutaryl-coenzyme A reductase and application of statins as a novel effective therapeutic approach against Acanthamoeba infections. *Antimicrobial agents and chemotherapy* **57**(1): 375-381.

Miziorko HM (2011) Enzymes of the mevalonate pathway of isoprenoid biosynthesis. *Arch Biochem Biophys* **505**(2): 131-143.

Mizranita V and Pratisto EH (2015) Statin-associated ocular disorders: the FDA and ADRAC data. *International journal of clinical pharmacy* **37**(5): 844-850.

Morck C, Olsen L, Kurth C, Persson A, Storm NJ, Svensson E, Jansson JO, Hellqvist M, Enejder A, Faergeman NJ and Pilon M (2009) Statins inhibit protein lipidation and induce the unfolded protein response in the non-sterol producing nematode Caenorhabditis elegans. *Proc Natl Acad Sci U S A* **106**(43): 18285-18290.

Muhlhauser U, Zolk O, Rau T, Munzel F, Wieland T and Eschenhagen T (2006) Atorvastatin desensitizes beta-adrenergic signaling in cardiac myocytes via reduced isoprenylation of G-protein gamma-subunits. *FASEB journal : official publication of the Federation of American Societies for Experimental Biology* **20**(6): 785-787.

Park D, Jhon DY, Lee CW, Lee KH and Rhee SG (1993) Activation of phospholipase C isozymes by G protein beta gamma subunits. *The Journal of biological chemistry* **268**(7): 4573-4576.

Pearring JN, Salinas RY, Baker SA and Arshavsky VY (2013) Protein sorting, targeting and trafficking in photoreceptor cells. *Prog Retin Eye Res* **36**: 24-51.

Pitcher J, Inglese J, Higgins J, Arriza J, Casey P, Kim C, Benovic J, Kwatra M, Caron M and Lefkowitz R (1992) Role of beta gamma subunits of G proteins in targeting the beta-adrenergic receptor kinase to membrane-bound receptors. *Science* **257**(5074): 1264-1267.

Ramkumar S, Raghunath A and Raghunath S (2016) Statin Therapy: Review of Safety and Potential Side Effects. *Acta Cardiol Sin* **32**(6): 631-639.

Reiter E and Lefkowitz RJ (2006) GRKs and beta-arrestins: roles in receptor silencing, trafficking and signaling. *Trends Endocrinol Metab* **17**(4): 159-165.

Ribas C, Penela P, Murga C, Salcedo A, García-Hoz C, Jurado-Pueyo M, Aymerich I and Mayor F (2007) The G protein-coupled receptor kinase (GRK) interactome: Role of GRKs in GPCR regulation and signaling. *Biochimica et Biophysica Acta (BBA) - Biomembranes* **1768**(4): 913-922.

Rodwell VW, Nordstrom JL and Mitschelen JJ (1976) Regulation of HMG-CoA reductase. *Advances in lipid research* **14**: 1-74.

Schmechel A, Grimm M, El-Armouche A, Hoppner G, Schwoerer AP, Ehmke H and Eschenhagen T (2009) Treatment with atorvastatin partially protects the rat heart from harmful catecholamine effects. *Cardiovascular research* **82**(1): 100-106.

Senarath K, Payton JL, Kankanamge D, Siripurapu P, Tennakoon M and Karunarathne A (2018) Ggamma identity dictates efficacy of Gbetagamma signaling and macrophage migration. *The Journal of biological chemistry* **293**(8): 2974-2989.

Senarath K, Ratnayake K, Siripurapu P, Payton JL and Karunarathne A (2016) Reversible G Protein betagamma9 Distribution-Based Assay Reveals Molecular Underpinnings in Subcellular, Single-Cell, and Multicellular GPCR and G Protein Activity. *Analytical chemistry* **88**(23): 11450-11459.

Shrivastava S, Pucadyil TJ, Paila YD, Ganguly S and Chattopadhyay A (2010) Chronic cholesterol depletion using statin impairs the function and dynamics of human serotonin(1A) receptors. *Biochemistry* **49**(26): 5426-5435.

Siripurapu P, Kankanamge D, Ratnayake K, Senarath K and Karunarathne A (2017) Two independent but synchronized Gbetagamma subunit-controlled pathways are essential for trailing-edge retraction during macrophage migration. *J Biol Chem* **292**(42): 17482-17495.

Sytkowski PA, Kannel WB and D'Agostino RB (1990) Changes in risk factors and the decline in mortality from cardiovascular disease. The Framingham Heart Study. *The New England journal of medicine* **322**(23): 1635-1641.

Tang X, Sun Z, Runne C, Madsen J, Domann F, Henry M, Lin F and Chen S (2011) A critical role of Gbetagamma in tumorigenesis and metastasis of breast cancer. *The Journal of biological chemistry* **286**(15): 13244-13254.

Tilley DG and Rockman HA (2006) Role of beta-adrenergic receptor signaling and desensitization in heart failure: new concepts and prospects for treatment. *Expert review of cardiovascular therapy* **4**(3): 417-432.

van Koppen CJ and Jakobs KH (2004) Arrestin-Independent Internalization of G Protein-Coupled Receptors. *Molecular Pharmacology* **66**(3): 365-367.

Vazquez-Prado J, Bracho-Valdes I, Cervantes-Villagrana RD and Reyes-Cruz G (2016) Gbetagamma Pathways in Cell Polarity and Migration Linked to Oncogenic GPCR Signaling: Potential Relevance in Tumor Microenvironment. *Molecular pharmacology* **90**(5): 573-586.

Wang M and Casey PJ (2016) Protein prenylation: unique fats make their mark on biology. *Nat Rev Mol Cell Biol* **17**(2): 110-122.

Watson AJ, Katz A and Simon MI (1994) A fifth member of the mammalian G-protein beta-subunit family. Expression in brain and activation of the beta 2 isotype of phospholipase C. *The Journal of biological chemistry* **269**(35): 22150-22156.

Wedegaertner PB, Wilson PT and Bourne HR (1995) Lipid modifications of trimeric G proteins. *The Journal of biological chemistry* **270**(2): 503-506.

Whyte DB, Kirschmeier P, Hockenberry TN, Nunez-Oliva I, James L, Catino JJ, Bishop WR and Pai JK (1997) K- and N-Ras are geranylgeranylated in cells treated with farnesyl protein transferase inhibitors. *The Journal of biological chemistry* **272**(22): 14459-14464.

Wong WW, Dimitroulakos J, Minden MD and Penn LZ (2002) HMG-CoA reductase inhibitors and the malignant cell: the statin family of drugs as triggers of tumor-specific apoptosis. *Leukemia* **16**(4): 508-519.

Yim YY, McDonald WH, Hyde K, Cruz-Rodríguez O, Tesmer JJG and Hamm HE (2017) Quantitative Multiple-Reaction Monitoring Proteomic Analysis of Gβ and Gγ Subunits in C57Bl6/J Brain Synaptosomes. *Biochemistry* **56**(40): 5405-5416.

Yu R, Longo J, van Leeuwen JE, Mullen PJ, Ba-Alawi W, Haibe-Kains B and Penn LZ (2018) Statin-Induced Cancer Cell Death Can Be Mechanistically Uncoupled from Prenylation of RAS Family Proteins. *Cancer research* **78**(5): 1347-1357.

Molecular Pharmacology Fast Forward. Published on February 14, 2019 as DOI: 10.1124/mol.118.114710
This article has not been copyedited and formatted. The final version may differ from this version.

Footnotes

Research reported in this publication was partially supported by the University of Toledo and National Institutes of Health-National Institute of General Medical Sciences, grant number [1R15GM126455-01A1].

Molecular Pharmacology Fast Forward. Published on February 14, 2019 as DOI: 10.1124/mol.118.114710
This article has not been copyedited and formatted. The final version may differ from this version.

Legends for Figures

Figure 1.

G protein prenylation and fluvastatin induced inhibition of Gβ1γ localization on the PM. (A) Major steps of the hepatic cholesterol biosynthesis/mevalonate pathway. By inhibiting the rate-limiting step enzyme; HMG-CoA reductase, statins reduce biosynthesis of many lipids including cholesterol. (B) Quantification of statin-mediated inhibition of G protein PM localization in living cells. Images of HeLa cells expressing Gβ1-YFP. Cells treated with 2 μM fluvastatin exhibited a complete cytosolic distribution of Gβ1, while the control cells showed primarily PM and IM-localized Gβ1-YFP. Cartoon shows how the line-profile data was obtained to calculate the G proteins distribution ratio ($F_{PM/Cytosol}$) in control and fluvastatin treated cells. Bar graph shows a $F_{PM/Cytosol} < 1.0$ for fluvastatin treated cells since Gβ1 is cytosolic, likely due to lack of prenylation (error bars: SEM, n=12 cells, $p < 0.05$). (C) Left: GPCR activation induced translocation of Gβγ dimer from the PM to IMs. In GPCR-inactive state, G protein heterotrimers reside on the PM and upon activation, heterotrimers dissociate, generating Gα-GTP and free Gβγ. The resultant Gβγ then can translocate from the PM to IMs in a Gγ-type dependent manner. Middle: Images show translocation of Gβ1 in control HeLa cells upon activation of endogenous α2-AR with 100 μM norepinephrine (NE). Fluvastatin treated cells exhibited ~50% attenuated translocation. Right: The plot shows the translocation dynamics of Gβ1. Yellow arrow indicate translocated Gβ1 on IMs (scale: 5 μm, error bars: SEM, n=20 cells, two tailed t-test was performed after the time point the response reached equilibrium and the data are statistically significant at 0.0001 level).

Figure 2.

Fluvastatin differentially attenuates the PM localization of Gγ9 and Gγ3. (A) Images of control cells pretreated with the carrier solvent (DMSO) exhibited a clear distribution of GFP-Gγ9 on the PM, indicating prenylated Gγ9. Fluvastatin treated cells showed near-complete cytosolic GFP-Gγ9, suggesting a complete

Molecular Pharmacology Fast Forward. Published on February 14, 2019 as DOI: 10.1124/mol.118.114710
This article has not been copyedited and formatted. The final version may differ from this version.

inhibition of Gγ9 prenylation. +Flu + Mevalonate cells show that supplementation of mevalonate abrogates fluvastatin action. Bar graph show that of +Flu-cells with $F_{PM/Cytosol} \leq 1$, exhibiting lack of GFP fluorescence on the PM while both Control and +Flu + Mevalonate cells with $F_{PM/Cytosol} > 1$ indicating the PM-bound GFP fluorescence. Images (left) and the plot show endogenous α2-AR activation mediated Gγ9 translocation only in Control and +Flu + Mevalonate cells. t-statistics show that at $p < 0.05$, mean $F_{PM/Cytosol}$ are not significantly different for control and +Flu +Mevalonate cells. In contrast, translocation in fluvastatin treated cells was significantly attenuated, indicating lack of PM-bound heterotrimers (error bars: SEM, n=12 cells, two tailed t-test was performed after the time point the response reached equilibrium and the data are statistically significant at 0.05 level). (B) Partial prenylation inhibition of GFP-Gγ3 in HeLa cells. Similar to GFP-Gγ9 expressing cells, Control and +Flu + Mevalonate cells showed that GFP-Gγ3 is on the PM. In contrast to Gγ9, +Flu-cells showed GFP-Gγ3 distribution only on the PM while no Gγ3 residing in IMs is observed. Upon endogenous α2-AR activation, cell in all three conditions exhibited translocation. The plot (right) shows a ~1/3-magnitude lower translocation in +Flu cells compared to control and +Flu + Mevalonate cells. This indicates that fluvastatin can attenuate Gβγ3 activation. Yellow arrows indicate Gβγ translocated to IMs (scale: 5 μm, error bars: SEM, n=15 cells, two tailed t-test was performed after the time point the response reached equilibrium and the data are statistically significant at 0.05 level).

Figure 3.

Fluvastatin has distinct inhibition abilities of membrane localization of Gγ1, Gγ2, Gγ4, and Gγ5. HeLa cells expressing (A) YFP-Gγ1 (B), YFP-Gγ2 (C), YFP-Gγ4 (D) and YFP-Gγ5 (E), pretreated overnight with 2 μM fluvastatin during transfection. Control cells showed a clear localization of Gγ on the PM and in IMs. Fluvastatin treated cells showed a complete cytosolic distribution of Gγ1. Gγ2, Gγ4, and Gγ5 transfected cells exposed to fluvastatin showed only a partial presence of YFP in the cytosol, similar

Molecular Pharmacology Fast Forward. Published on February 14, 2019 as DOI: 10.1124/mol.118.114710
This article has not been copyedited and formatted. The final version may differ from this version.

to GFP-Gγ3 cells exposed to fluvastatin. Bar graphs show $F_{PM/Cytosol}$ in control and +Flu cells in which Gγ1, Gγ2 and Gγ4 show a significant increase in cytosolic YFP compared control cells. However, no significant difference in $F_{PM/Cytosol}$ of Gγ5 cells was observed between control and +Flu conditions. (scale: 5 μm, error bars: SD, $10 < n < 15$ cells, $p < 0.05$).

Figure 4.

Different statins show distinct inhibitions of the PM localization of the same G protein. (A) Compared to fluvastatin treated cells, HeLa cells expressing GFP-Gγ9 and GFP-Gγ3 treated with either lovastatin or atorvastatin only exhibited a minor inhibition of the Gγ-PM localization . The plot shows percentage of cells showed at least partial membrane localization inhibition in the GFP-Gγ expressing cell populations. Symbols ■, ⋆ and ● on the plot indicate complete, moderate, and minor inhibitions respectively ($10 < n < 30$ cells). A two-way ANOVA shows that Gγ3 and Gγ9 significantly differ, F (1,12) = 41.2, $p < 0.05$, such that the average inhibition was significantly higher for Gγ9 (M = 51.2%, SEM = 10.8) than for Gγ3 (M = 22.8%, SEM = 5.4). The inhibitory effect on Gγ membrane interactions of drugs were also significant, F (2, 12) = 63.2, $p > 0.05$ such that +Flu effect was significantly higher (M = 74.6%, SEM = 10.5), compared to Ator (M = 28.1%, SEM = 7.5) and Lov (M = 19.0%, SEM = 3.4). (B) HeLa cells expressing mCh-KRas and mCh-MRas pre-treated with either DMSO (control) or fluvastatin. Compared to control cells, both KRas and MRas in +Flu cells showed a complete cytosolic fluorescence distribution, indicating the near-complete inhibition of their farnesylation. Bar graph (middle) with $F_{PM/Cytosol}$ indicates significant differences in inhibitions between control and +Flu cells in both KRas and MRas cells. Bar graph (right) with % number of cell with PM localization. +Flu shows effective inhibitions of both Ras members while atorvastatin shows ~40% inhibition of MRas and near zero inhibition of KRas. + Lov exhibited minor inhibition of both Ras members (scale: 5 μm, error bars: SEM, n=17 cells, $p < 0.05$). (C) HeLa cells expressing GFP-Rac1 showed a clear PM localization

Molecular Pharmacology Fast Forward. Published on February 14, 2019 as DOI: 10.1124/mol.118.114710
This article has not been copyedited and formatted. The final version may differ from this version.

while in +Flu cells showed GFP fluorescence primarily in the nucleus. Interestingly, +Lov and +Ator treatments induced bi-phasic responses, i.e. only a fraction of cell population exhibited a complete nuclear localization of Rac1. (scale: 5 μm, error bars: SEM, $n \geq 15$ cells, $p < 0.05$)

Figure 5.

Fluvastatin perturbs Gβγ signaling in RAW 264.7 macrophages. (A) Upon activation of endogenous c5a receptor with 20 μM c5a, 55% of control (DMSO treated) RAW 264.7 cells exhibited increase in fluo-4 fluorescence (green), indicating cellular calcium increase. On the contrary, only ~11% of 10 μM fluvastatin treated cells showed weaker calcium responses. The plot compares representative calcium responses by a control and +Flu cell. Bar graph shows that, compared to control cells, +Flu, +Ator and +Lov treated cells exhibited varying levels of calcium response inhibitions. However, responses observed +Ator cells were not significantly different from that of control cells (scale bar: 10 μm, number of fields ≥ 6, $n < 30$ cells in each field, error bars: SD, $p < 0.05$). (B) RAW 264.7 cells expressing blue opsin-mTurquoise (Gi-coupled GPCR), Akt-PH-mCh (PIP3 sensor), and either GFP-GPI or GFP-Gγ3 pre-incubated with 50 μM 11-*cis*-retinal. Both WT Control and GFP-Gγ3 cells showed PIP3 generation, indicated by the translocation of cytosolic Akt-PH-mCh to the PM (Yellow arrow). Fluvastatin exhibited the highest inhibition in both WT Control and GFP-Gγ3 expressing cells. Plots and a two-way ANOVA showed that, the PIP3 production inhibition by all three drugs are statistically significant. (scale bar: 5 μm, error bars: SEM, $n \geq 15$ cells, $p < 0.05$).

Figure 6.

Fluvastatin attenuates Gi-pathway governed cell migration, invasion and reduces Akt phosphorylation. (A) A RAW 264.7 cell expressing blue opsin-mTurquoise and Akt-PH-mCh and incubated with 50 μM 11-*cis*-retinal exhibited a directional migration towards the optical stimuli upon localized optical activation of blue opsin (blue box). This migration is accompanied with lamellipodia and

Molecular Pharmacology Fast Forward. Published on February 14, 2019 as DOI: 10.1124/mol.118.114710
This article has not been copyedited and formatted. The final version may differ from this version.

clear generation of PIP3 at the leading edge. In contrast, cells treated with 10 μM fluvastatin exhibited a significant reduction ($p<0.05$) in cell migration, lamellipodia formation, and PIP3 generation (error bars: SD, n> 10 cells, $p < 0.05$). (B) Bar graph shows invasion of RAW 264.7 cells in the transwell invasion assay, induced by endogenous c5a receptor activation using 12.5 μM c5a. Compared to control (DMSO) cells, fluvastatin, RhoA inhibitors (EHop-016, EHT1864, and GSK269962), and PI3K inhibitor (wortmannin) treated cells exhibited significant reductions in cell invasion (n=2). Compared to wortmannin treated cells, fluvastatin treated cells exhibited ~50% more inhibition, indicating that inhibition through fluvastatin can be due to prenylation inhibition of both Gγ as well as Ras family proteins (error bars: SD, n< 3 independent experiments, $p<0.05$). (C) Examination of Akt phosphorylation in cells exposed to fluvastatin using Western blot analysis. Images and bar graph show ~ 40% less Akt phosphorylation in +Flu cells, compared to control cells. Protein expressions were normalized to both total Akt and β-Actin. (error bars: SD, n= three independent experiments, $p< 0.05$).

Figure 7.

Fluvastatin (A) attenuates internalization of activated β1-adrenergic receptors in HeLa cells, and (B) impairs Gβγ-mediated signaling in ARPE-19 cells. (A) The schematic representation of Nb80 translocation to activated β1-AR and its subsequent internalization with the receptor. Images show the Nb80-GFP movement in HeLa cells expressing β1-AR-CFP upon receptor activation. After activation of β1-AR with 20 μM isoproterenol, control cells showed a robust recruitment of Nb80 (both GFP and mCh tagged) to the IMs with the internalized and active β1-AR (top image panel, yellow arrows). A comparatively reduced Nb80 recruitment was observed in +Flu cells (second panel right, white arrow). The plot shows ~ 50% reduced mean GFP fluorescence of Nb80 in the IMs in fluvastatin treated cells indicating attenuated β1-AR desensitization (n = 20 cells from 4 independent experiments). Both 10 μM gallein (Gβγ inhibitor) treated cells (third panel right, white arrow) and membrane targeted venus-GRK3ct (mask Gβγ) expressing cells showed ~80% lower Nb80 accumulation in IMs (white arrows), indicating

the involvement of Gβγ in the pathway. Both Nb80-GFP and -mCh versions exhibited similar internalization in control cells (red and black curves respectively). (B) Real time PCR quantification of relative expression levels of the twelve Gγ subtypes in ARPE-19 cells. Farnesylated Gγ11 showed the highest expression. Images show ARPE-19 cells expressing blue opsin-mTurquoise either with Gβ1-mCh or mCh-Gγ9 and incubated with 50 μM 11-*cis*-retinal. Gβ1 and Gγ9 in control cells were primarily found on the PM (white arrows) and upon blue opsin activation both proteins exhibited robust translocations from the PM to IMs (yellow arrows). Likely due to prenylation inhibition, both Gβ1 as well as Gγ9 distribution in +Flu cells were completely cytosolic and their translocations upon blue opsin activation were not detected. Collectively, these data indicate the lack of prenylation of endogenous Gγ types as well as transfected Gγ9 upon fluvastatin treatment**.** (scale: 5 μm, error bars: SEM, n = 16 cells, $p < 0.05$).

Figures

Figure 1

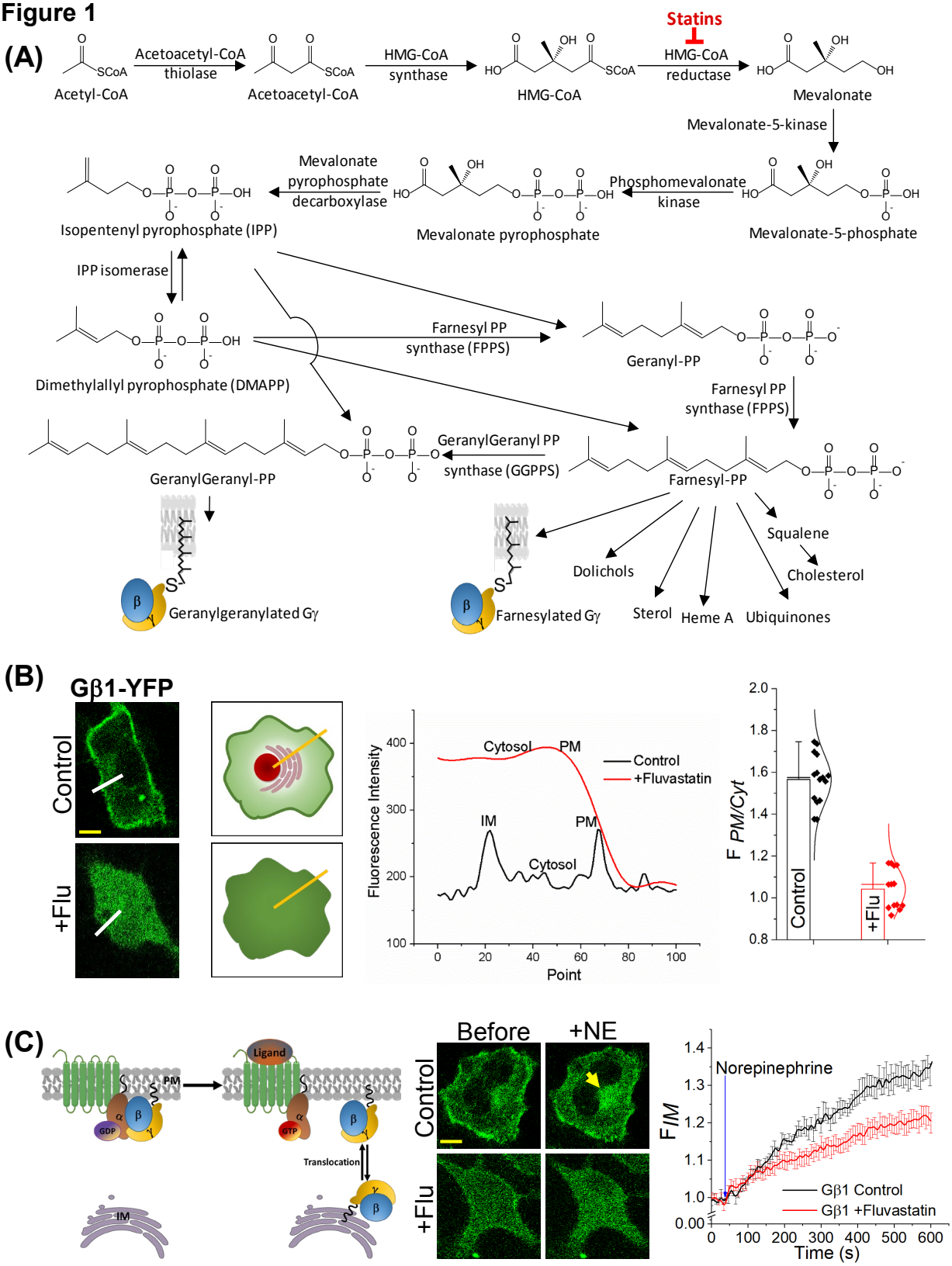

Figure 2

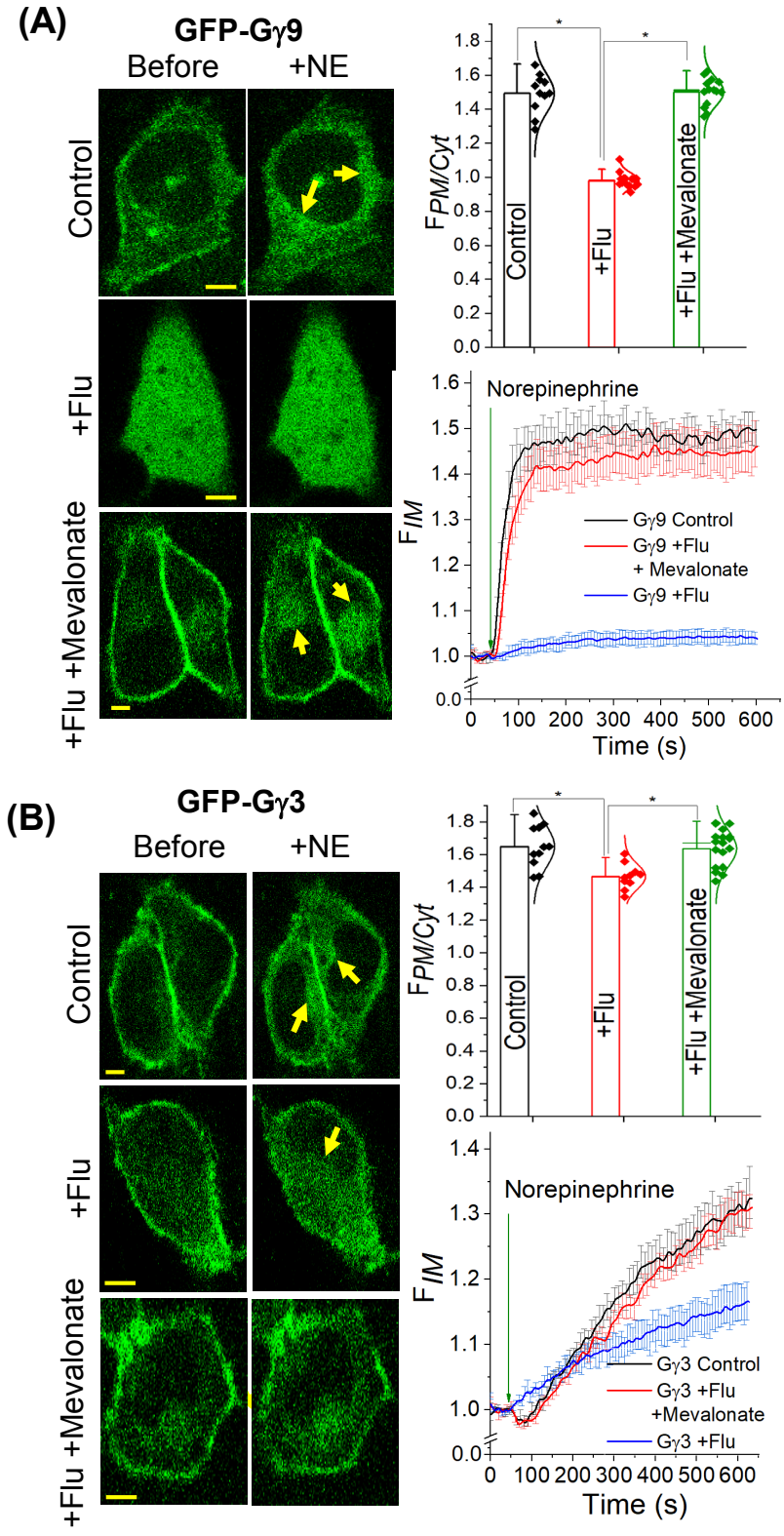
(A)
GFP-Gγ9
Before
+NE
Control
+Flu
+Flu +Mevalonate
F PM/Cyt
Control
+Flu
+Flu +Mevalonate
Norepinephrine
F IM
Gγ9 Control
Gγ9 +Flu
+ Mevalonate
Gγ9 +Flu
Time (s)
(B)
GFP-Gγ3
Before
+NE
Control
+Flu
+Flu +Mevalonate
F PM/Cyt
Control
+Flu
+Flu +Mevalonate
Norepinephrine
F IM
Gγ3 Control
Gγ3 +Flu
+Mevalonate
Gγ3 +Flu
Time (s)

Figure 3

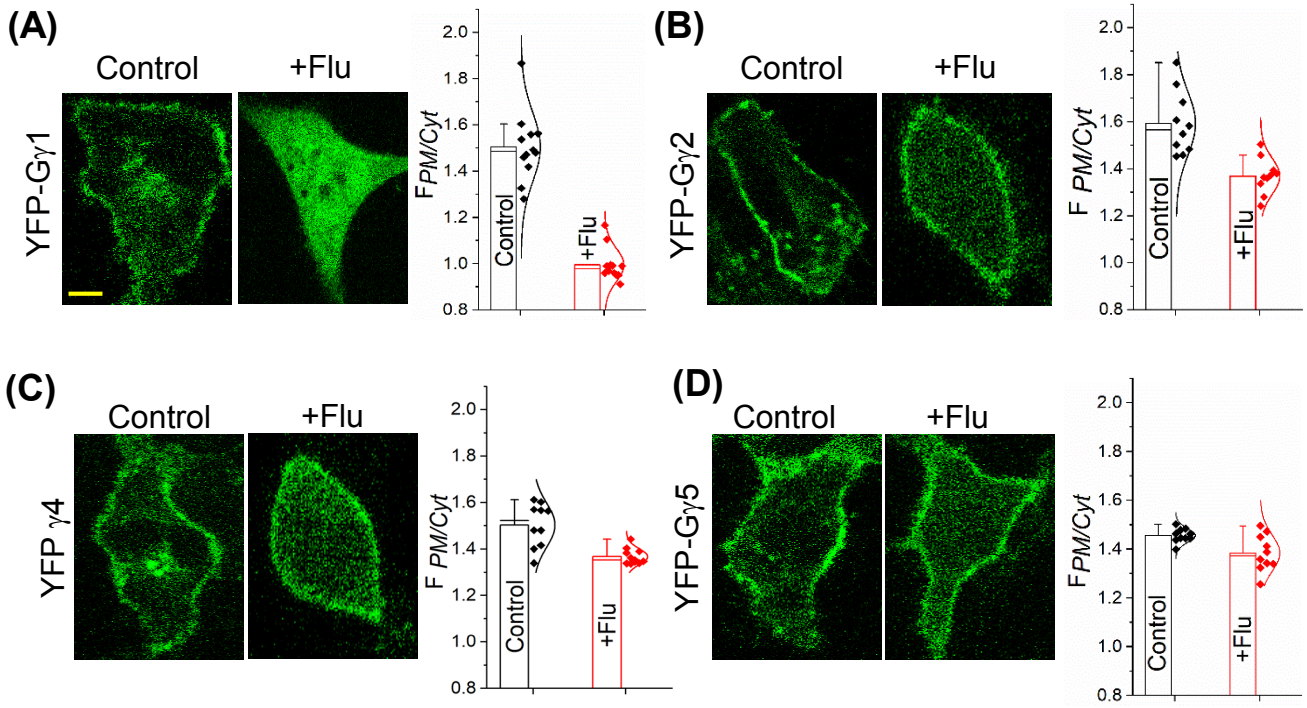
(A)
Control
+Flu
YFP-Gγ1
F PM/Cyt
Control
+Flu
(B)
Control
+Flu
YFP-Gγ2
F PM/Cyt
Control
+Flu
(C)
Control
+Flu
YFP γ4
F PM/Cyt
Control
+Flu
(D)
Control
+Flu
YFP-Gγ5
F PM/Cyt
Control
+Flu

Figure 4

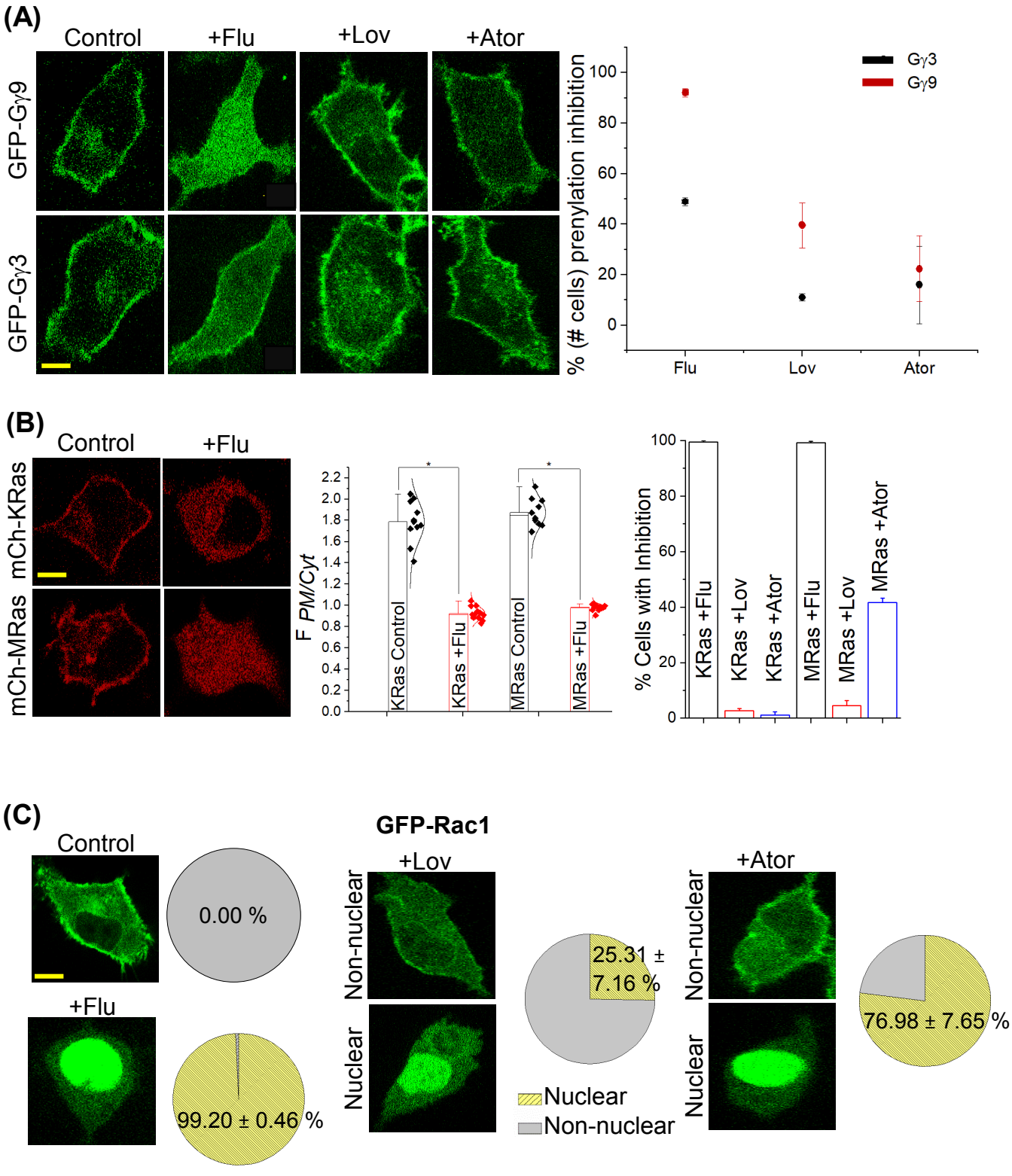
(A)
Control
+Flu
+Lov
+Ator
GFP-Gγ9
GFP-Gγ3
% (# cells) prenylation inhibition
Gγ3
Gγ9
Flu
Lov
Ator
(B)
Control
+Flu
mCh-KRas
mCh-MRas
F PM/Cyt
KRas Control
KRas +Flu
MRas Control
MRas +Flu
% Cells with Inhibition
KRas +Flu
KRas +Lov
KRas +Ator
MRas +Flu
MRas +Lov
MRas +Ator
(C)
Control
+Flu
0.00 %
99.20 ± 0.46 %
GFP-Rac1
+Lov
+Ator
Non-nuclear
Nuclear
25.31 ± 7.16 %
76.98 ± 7.65 %
Nuclear
Non-nuclear

Figure 5

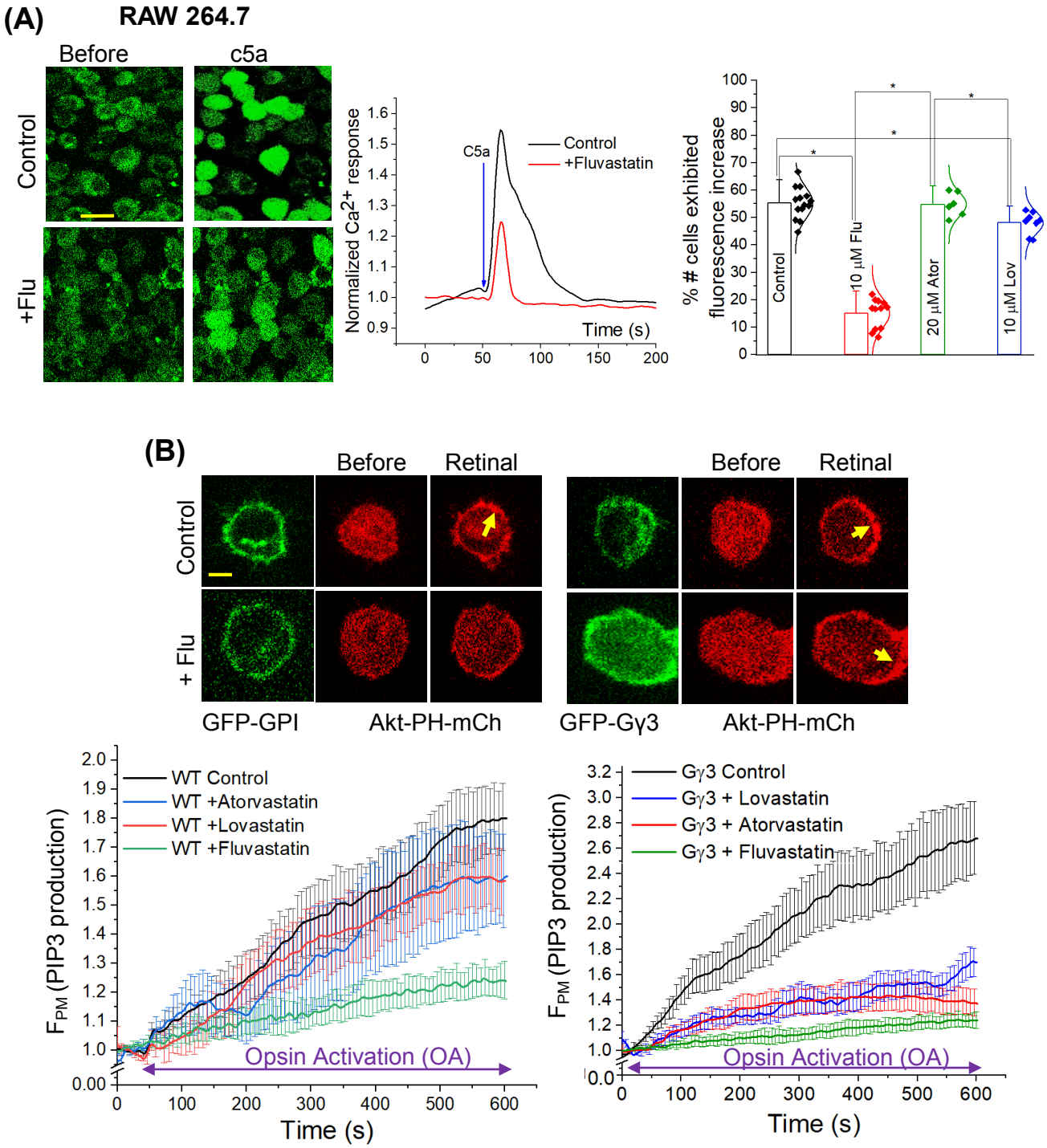
(A)
RAW 264.7
Before
c5a
Control
+Flu
Normalized Ca2+ response
C5a
Control
+Fluvastatin
Time (s)
% # cells exhibited fluorescence increase
Control
10 μM Flu
20 μM Ator
10 μM Lov
(B)
Before
Retinal
Control
+ Flu
GFP-GPI
Akt-PH-mCh
GFP-Gγ3
Akt-PH-mCh
WT Control
WT +Atorvastatin
WT +Lovastatin
WT +Fluvastatin
FPM (PIP3 production)
Opsin Activation (OA)
Time (s)
Gγ3 Control
Gγ3 + Lovastatin
Gγ3 + Atorvastatin
Gγ3 + Fluvastatin
FPM (PIP3 production)
Opsin Activation (OA)
Time (s)

Figure 6

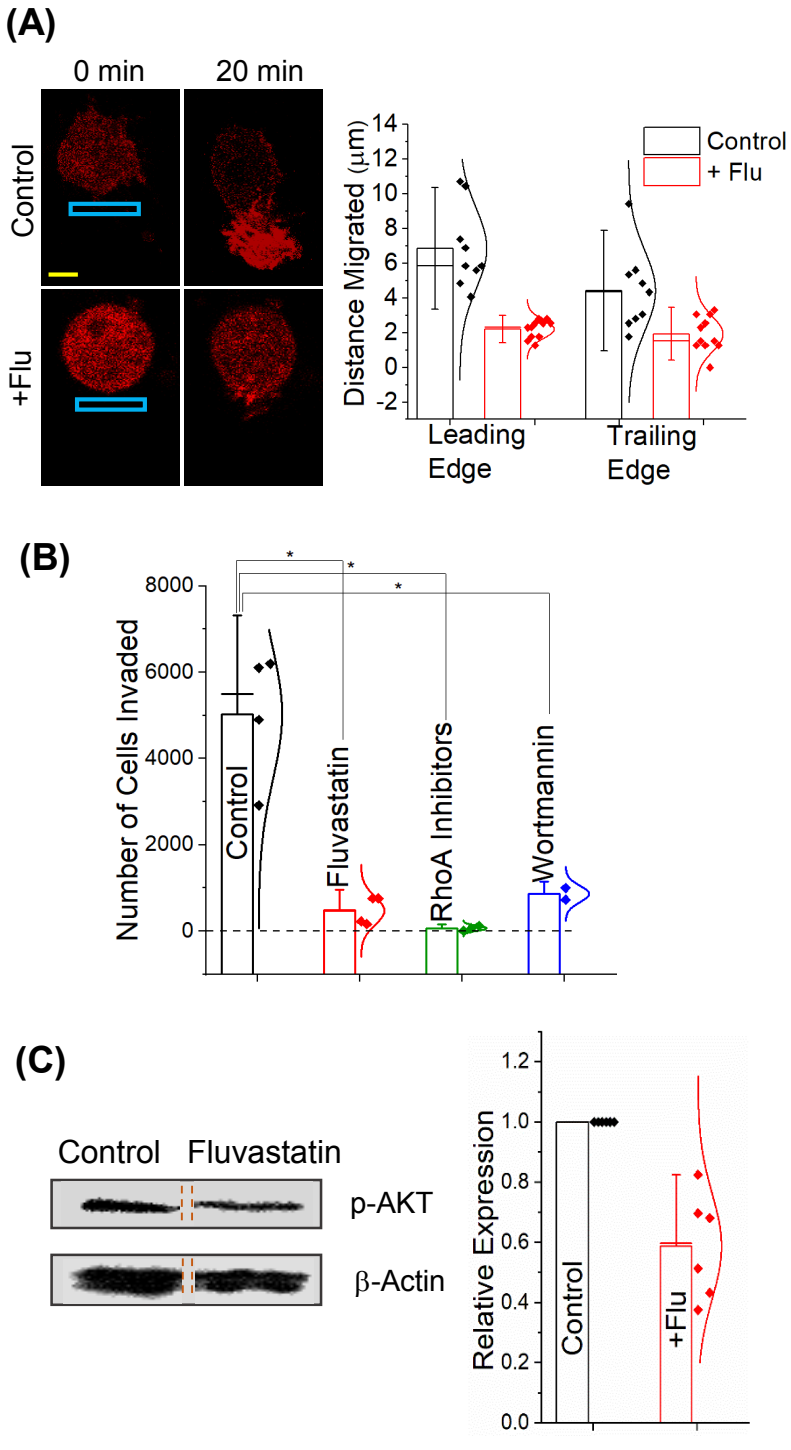
(A)
0 min
20 min
Control
+Flu
Distance Migrated (μm)
14
12
10
8
6
4
2
0
-2
Control
+ Flu
Leading Edge
Trailing Edge
(B)
Number of Cells Invaded
8000
6000
4000
2000
0
*
*
*
Control
Fluvastatin
RhoA Inhibitors
Wortmannin
(C)
Control
Fluvastatin
p-AKT
β-Actin
Relative Expression
1.2
1.0
0.8
0.6
0.4
0.2
0.0
Control
+Flu

Figure 7

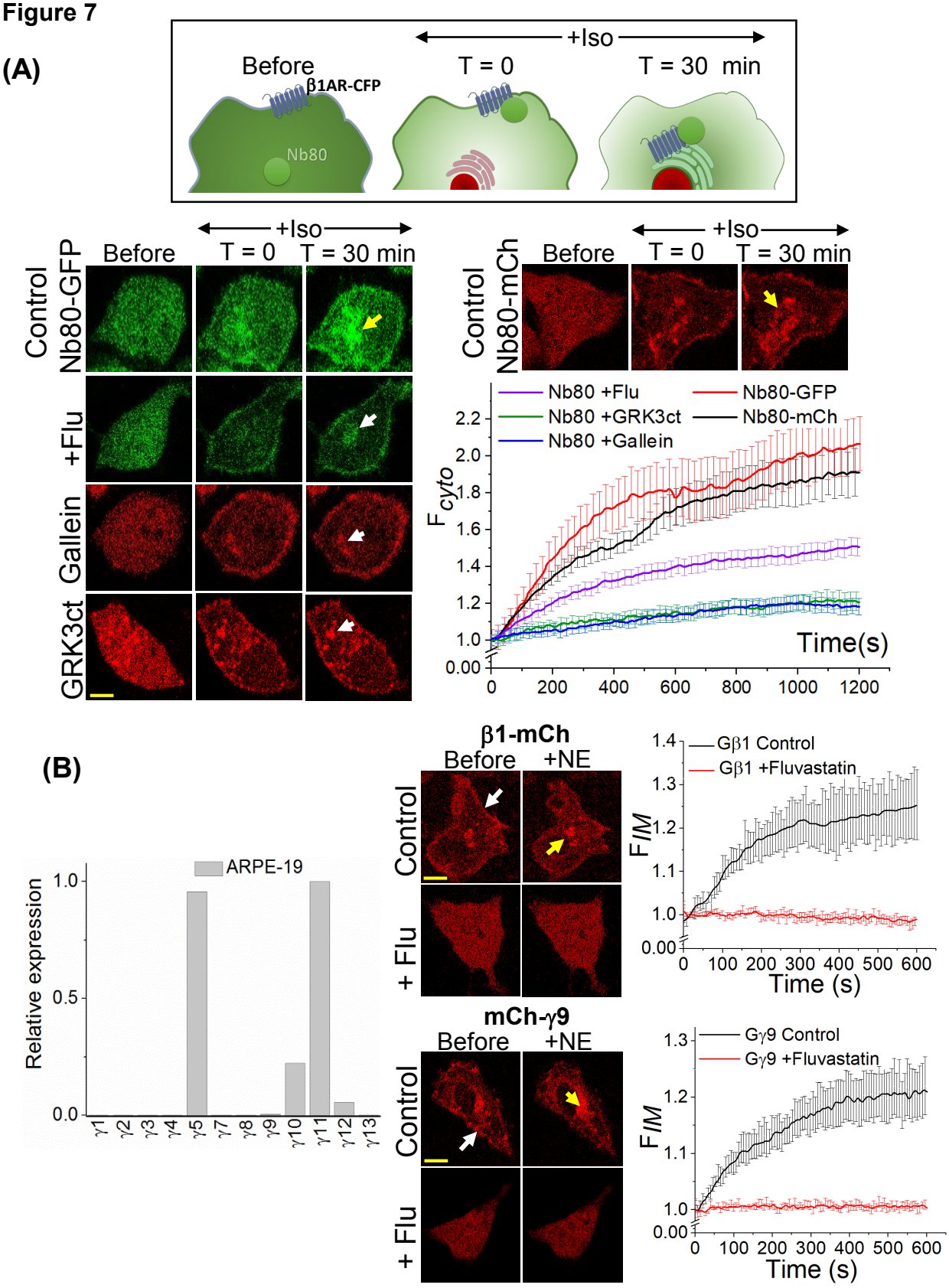
(A)
+Iso
Before
T = 0
T = 30 min
β1AR-CFP
Nb80
Control
Nb80-GFP
+Flu
Gallein
GRK3ct
Nb80-mCh
Nb80 +Flu
Nb80 +GRK3ct
Nb80 +Gallein
Nb80-GFP
Nb80-mCh
F cyto
Time(s)
(B)
ARPE-19
Relative expression
β1-mCh
+NE
+ Flu
Gβ1 Control
Gβ1 +Fluvastatin
F IM
Time (s)
mCh-γ9
Gγ9 Control
Gγ9 +Fluvastatin

Supplemental Data

Statins perturb Gβγ signaling and cell behavior in a Gγ subtype dependent manner

Mithila Tennakoon, Dinesh Kankanamge, Kanishka Senarath, Zehra Fasih and Ajith Karunarathne

Molecular Pharmacology

Supplemental Figure Legends

Supplemental Figure 1

A) **Comparison of cellular distribution of WT mCh-Gγ3 with and without +Flu and mCh-Gγ3 (C72A) mutant.** While WT mCh-Gγ3 expressing control cells showed a strong distribution of Gγ3 on both PM and IMs, +Flu cells having lost their ability to bind to IM exhibited Gγ3 only on the PM (Yellow arrow). Comparatively mCh-Gγ3(C72A) mutant expressing cells showed Gγ3 distribution all over the cytosol, but not bound to either PM or IMs (scale bar: 5 μm).

B) **Comparison of the extents of Gγ membrane binding inhibition by fluvastatin.** As the numerical value indicates, while farnesylated Gγ1 exhibited the highest inhibition, the other geranylgeranylated Gγs showed comparatively low inhibition. One-way ANOVA was performed, and the data were statistically different F (4, 77) = 79.19, P<0.05 (error bars: SD, n > 10, p < 0.05).

C) **Gγ-type independent inhibition of IM binding by fluvastatin.** HeLa cells expressing CFP-KDEL and either mCh-Gγ9 or Gγ3. Compared to control cells of both Gγ9 and Gg3 with clear distribution of Gγ bound to IMs (yellow arrow), regardless of the Gγ subtype, +Flu cells exhibited absence of Gγ on the IMs. CFP-KDEL shows the intact IMs even after +Flu treatment to cells (scale bar: 5 μm)

D) **Effects of fluvastatin treatment on subcellular distribution of heterotrimeric G protein subunits.** HeLa cells expressing Gαo-CFP, Gβ1-mCh, and Gg9-YFP. Compared to control cells, PM localization of Gαo subunit of many +Flu cells remained intact. However, both Gβ1 and Gγ9 showed primarily a cytosolic distribution (scale bar: 5 μm).

E) **The varying effect of Gγ3 and Gγ9 translocation from PM to IM by different drug.** Plots shows the extent of translocation of Gγ9 (left) and Gγ3 (right) with different drug treatment. Compared to the effect on +Flu cells, in the Gγ9 and Gg3 expressing cells the effect by +Ator and +Lov is moderate. (error bars: SEM, n > 12, p < 0.05)

Supplemental Figure 2

A) **Comparison of prenylation-inhibition by fluvastatin and farnesyl transferase inhibitor, Lonafarnib.** Hela cells expressing GFP-Gγ9 and GFP-Rac1 exhibited identical and complete inhibitions of PM-binding when exposed to fluvastatin and lonafarnib, indicating that both inhibit farnesylation (scale bar: 5 μm).

B) The original images of Western blot analysis showing the expression of p-Akt and β-Actin with and without Fluvastatin. The yellow dashed line indicates the spliced-border where the band splicing was done in the main figure, due to merging of bands.

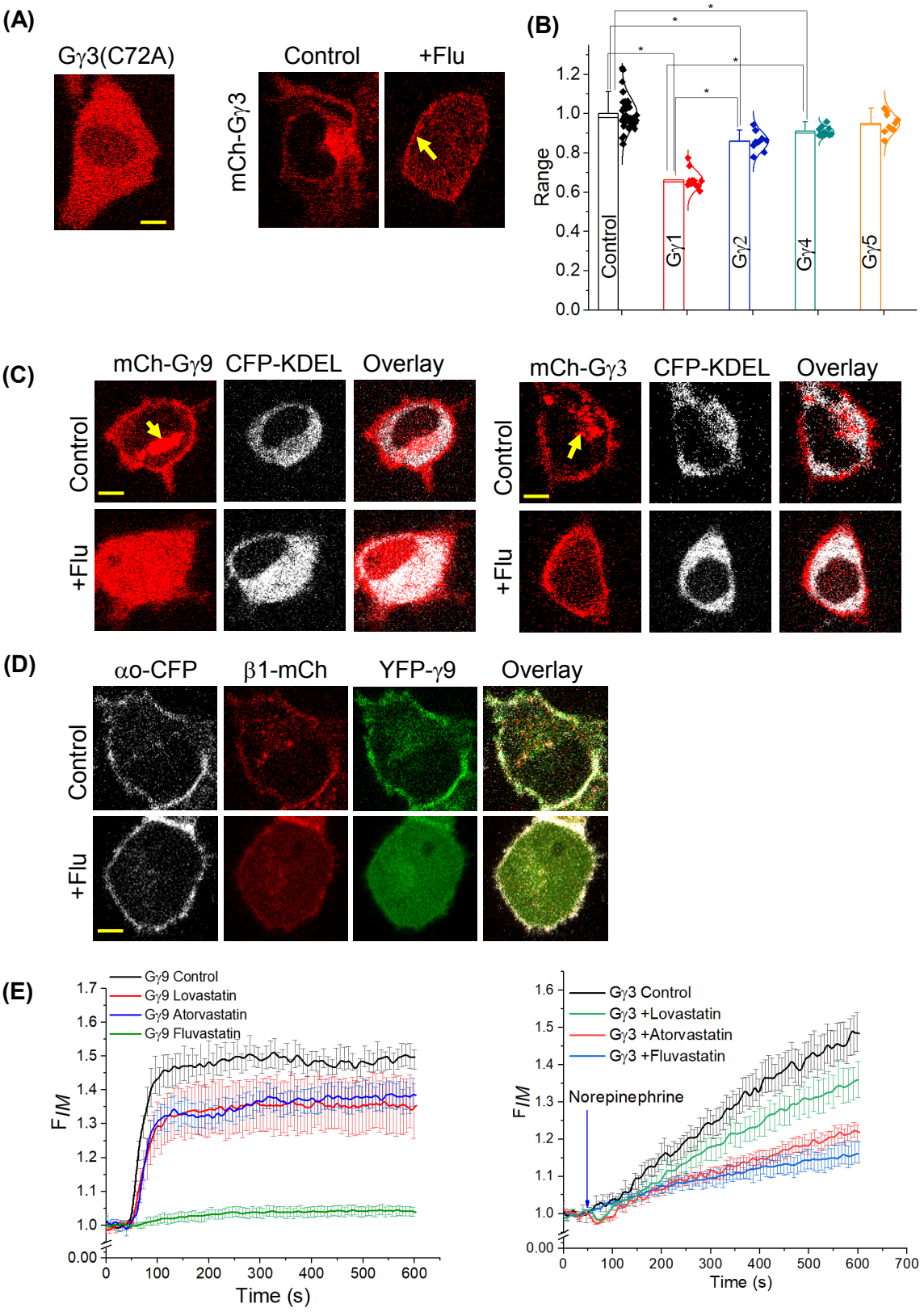

Supplemental Figure 1

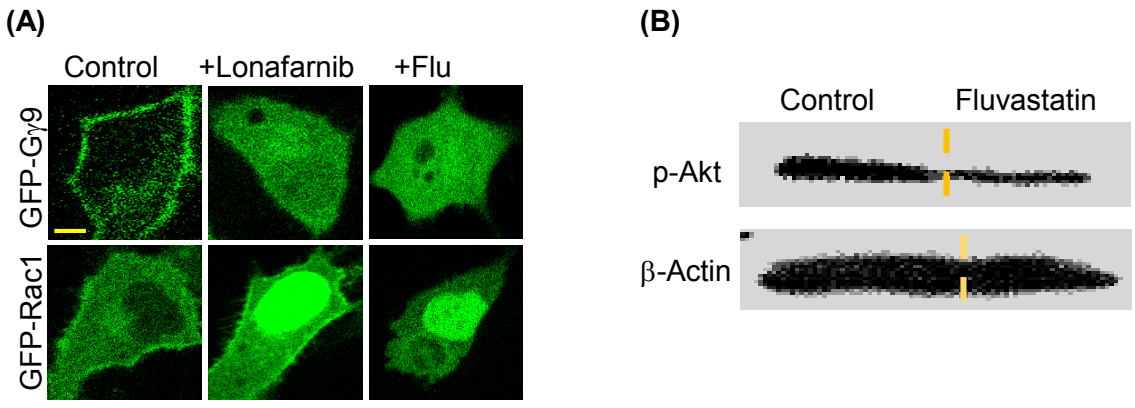

Supplemental Figure 2